國立台灣大學醫學院微生物學研究所
碩士論文

Graduate Institute of Microbiology
College of Medicine
National Taiwan University
Master Thesis

肺炎鏈球菌 NanA 誘導之去唾液酸化對於 Siglec-Toll-like receptor 交互作用之影響

Impact of pneumococcal NanA-mediated host desialylation in Siglec-Toll-like receptor crosstalk

張鈞棋

Chun-Chi Chang

指導教授：張永祺 博士

Advisor: Yung-Chi Chang, Ph.D.

中華民國 106 年 7 月

July 2017

doi:10.6342/NTU201701774

國立臺灣大學（碩）博士學位論文
口試委員會審定書

中文題目：肺炎鏈球菌 NanA 誘導之去唾液酸化對於 Siglec-Toll-like receptor 交互作用之影響

英文題目：Impact of pneumococcal NanA-mediated host desialylation in Siglec-Toll-like receptor crosstalk

本論文係 張鈞棋 君（學號 r04445114）在國立臺灣大學微生物學所完成之碩（博）士學位論文，於民國 106 年 7 月 6 日承下列考試委員審查通過及口試及格，特此證明

口試委員：

張永祺 （簽名）

（指導教授）

系主任、所長 鄭逸寧 （簽名）

doi:10.6342/NTU201701774

致謝

一眨眼，在台大微生物所的兩年碩士生活就這樣充實且匆忙的結束了，一路上遇到太多人，發生太多事而讓兩年的北漂生活添增了許多色彩；若沒有這麼多的人在這段旅程中伸出援手，一個人的力量絕對不可能這樣順利的完成碩士學業。

我的指導老師張永祺老師，非常感謝這兩年來老師提供了一個這麼舒適又自在的實驗環境讓我很自由的發揮所長，在實驗室裡大家一起努力向上做研究，拚實驗、趕進度，一起完成了碩士生涯中大大小小的報告；很感謝老師在實驗上不管是設計、邏輯或是操作上的指導，我真的學到很多東西，當中論文的撰寫也受益良多，希望老師能趕快 paper 大發升等副教授。R1418 的實驗夥伴們，很謝謝大家在實驗上的互相幫助、打屁聊天而讓這些許枯燥的研究生活不那麼無聊；謝謝曜誠學長在我碩一時協助實驗起初建立的腳步，謝謝紹彗這兩年來一起打拼課業、報告、實驗、分享生活，謝謝逸萱和昭賢學弟妹在大小事上的幫忙，有你們讓實驗室更歡樂更有趣。

很重要地，謝謝董馨蓮老師讓我能在碩一時短暫的在貴實驗室學習與進步，老師對科學的熱忱與耐心是我很敬佩的；也謝謝董老師家的學長姊，俊賢學長、建麗學姊在我碩一時常常讓我煩，跟你們分享我的生活，即使你們畢業後也常常關心我的實驗或生活近況，真的很幸運也很開心能讓認識你們。

難能可貴的是從中國醫生科畢業後一起到台北讀書的”台北菸酒生”們，兩年來大大小小的抱怨、挫折、負能量都分享給彼此了；同樣地，在課業以及實驗上的交流分享、互享砥礪也是很珍貴，我想我一定會很懷念每次聚會開懷大笑的時光，而能把所有煩惱拋諸腦後，兩月一次共十二次的大聚伴我走過太多北漂的回憶，能有你們這樣一群朋友是我莫大的榮幸。

真正讓我走上科學這條不歸路的啟蒙老師-徐媛曼老師，謝謝您在五年前把什麼都不會的我撿進實驗室，讓我在裡面成長學習，讓我有紮實的基礎與獨立思考的能力，我的碩士學業能如期完成，老師的功勞絕對佔了很大一部分。也謝謝當初在實驗室打拼的夥伴，千香學姊、一毛學姊、phoebe 學姊、暐涵和家瑜，在我大學畢業後也一直保持聯絡給我實驗上的鼓勵與建議。

最後也最重要的是我的家人，雖然常抱怨我在這兩年內回家的次數越來越少間格越來越長，但心裡還是擔心我在台北有沒有吃飽、會不會累、考試或報告準備得怎麼樣、連口試委員的餐點都要關心，很謝謝你們一直在背後支持我的所有決定，現在我畢業了，也能讓你們驕傲了。

doi:10.6342/NTU201701774

中文摘要

肺炎鏈球菌是全球單一致死率最高的病原菌之一，其感染能造成廣泛的疾病，包含了鼻竇炎、中耳炎、肺炎、菌血症以及腦膜炎等。在臨床上即使抗生素成功的清除病原菌本身，肺炎鏈球菌感染所造成的死亡與其所引起免疫反應的失衡有很大的關係。所有已被鑑定的肺炎鏈球菌株中，都能夠表現唾液酸酶(NanA)在細菌的表面，我們先前的結果顯示肺炎鏈球菌 NanA 能夠藉由移除表現在相同細胞上 Siglec 受體的順配體進而加劇白血球的發炎反應。免疫系統的細胞表面填充了各式各樣的凝集素與聚醣，而 Siglec 受體的辨認位置通常會被同個細胞表面其他唾液酸聚醣的配體覆蓋；而先天免疫系統上唾液酸廣泛且大量的表現以及其相對應具有免疫抑制模組受體的重要性，因此唾液酸通常被認為是 self-associated molecular patterns 來調控免疫細胞啟動的閾值。類鐸受體為模式識別受體(pattern recognition receptors)的一員，被廣泛地認為是對抗病原菌的第一道防線，當感染時，免疫細胞表面的模式識別受體感應外在的刺激，並藉由細胞內的訊息傳導來整合並引發適當的免疫反應來對抗外在的感染源，在本篇研究中我們將探討肺炎鏈球菌 NanA 誘導之唾液酸化對於 Siglec 與模式識別受體之間交互作用的影響。我們假設在肺炎鏈球菌感染情況下，NanA 誘導的去唾液酸化會破壞類鐸受體以及 Siglec 之間的交互作用，使得類鐸受體下游的訊息傳遞失衡而產生大量的發炎物質。我們的結果顯示野生型的肺炎鏈球菌相比 NanA 缺失的肺炎鏈球菌更能引起腫瘤壞死因子-α 的表現，而腫瘤壞死因子-α 表現的增加仰賴部分細胞表面脂筏的構造以及一些參與在 MAPK、PI3K/AKT 以及 NF-κB 訊息路徑中分子的活化；這樣細胞活化過程，可能來自於類鐸受體-2 與 Siglec-5 交互作用以及 Siglec-5 相關調控分子受到影響的結果。除了探討肺炎鏈球菌 NanA 誘導的發炎反應中，抑制性 Siglec 所扮演的角色外，我們也發現當人類巨噬細胞以及單核球細胞表現促進性 Siglec 在表面時，也會影響肺炎鏈球菌 NanA 誘導發炎反應的結果。

關鍵詞：肺炎鏈球菌、唾液酸酶、類鐸受體-2、Siglec-5、Siglec-14

doi:10.6342/NTU201701774

Abstract

Streptococcus pneumoniae (SPN) is the single most deadly bacterial infection globally, capable of causing a wide spectrum of disease, including sinusitis, otitis media, pneumonia, bacteremia and meningitis. The mortality caused by pneumococcal disease is sometimes linked to imbalanced hyper-inflammatory responses of the host despite of successful pathogen clearance. All SPN strains identified so far produce a surface-associated sialidase (NanA) and we recently demonstrated that leukocyte inflammatory responses are aggravated by pneumococcal NanA through removing the *cis*-lignads of Siglec expressed on the same myeloid cells. Cell surface in the immune system are richly equipped with a complex mixture of various lectins and glycans. Siglec binding sites are typically 'masked' by *cis* interactions with other sialoglycan ligands expressed on the same cell. Given the ubiquitous and abundant expression of host Sias and the prominence of cognate ITIM-bearing receptors on innate immune cells, Sia is proposed to act as "self-associated molecular patterns" to control the activation threshold of immune cells. Toll-like receptor (TLR) family, a member of pattern recognition receptors (PRRs), are generally thought to be a first-line defense to recognize pathogens. Upon infection, immune cells sense the environment through their various PRRs, processing and integrating this external information through the intracellular signaling cascade and induce appropriate immune responses to combat infectious microbial agents. Thus, this study we aimed to further investigate how pneumococcal NanA-mediated cell desialylation affects the crosstalk between Siglec and PRR signaling pathway. We hypothesized NanA-mediated host cell desialylation may disrupt the interaction between TLR and Siglec, dysregulate the inflammatory signals downstream of TLR and cause excessive pro-inflammatory substance upon pneumococcal infection. Our data suggested that WT SPN was able to induce stronger TNF-α production that partially rely on lipid rafts structure on cell membrane and activation of signaling molecules involved in MAPK, PI3k/Akt and NF-κB pathways compared to Δ*nanA* SPN. This pneumococcal NanA-mediated cell activation may result from affecting TLR-2-Siglec-5 interaction and Sigelc-5-associated signaling molecules. In addition to dissect the role of inhibitory Siglec in NanA-mediated pneumococcal inflammation, we also found that expression of an activating Siglec, Siglec-14, on human primary macrophages and THP-1 cells also affects host immune responses upon cell surface desialylation by pneumococcal NanA.

Key words: *Streptococcus pneumoniae*, NanA, TLR-2, Siglec-5, Siglec-14

doi:10.6342/NTU201701774

Content

doi:10.6342/NTU201701774

I. Introduction

A. Streptococcal neuraminidase

Streptococcus pneumoniae (SPN), a Gram-positive bacterial pathogen, is one of the leading cause of community-acquired pneumonia. SPN is the normal flora colonizing on the mucosal surface of the host nasopharynx and is found in approximately 85% of children under the age of 4 years [1]. While this colonization is typically asymptomatic and self-limiting, it is the requisite step for most if not all pneumococcal diseases [2,3]. The common manifestation of pneumococcal diseases includes acute otitis media, pneumonia and meningitis [4]. Current pneumococcal vaccines are exclusively targeted at the SPN capsular polysaccharide, which provide strictly serotype-specific protection and result in the increase in the incidence of bacteremia caused by non-included serotypes [5-7].

During the progression of pathogenesis, bacterial pathogens evolve various sophisticated strategies to prevail over host immunity and compete against the microflora residing in the same niche. Streptococcal neuraminidase (Nan), also known as sialidase, is one of the exoglycosidases produced by SPN. SPN encodes at least three neuraminidase genes: *nanA*, *nanB* and *nanC*. All strains encode *nanA*, and most also encodes *nanB*; however, only approximately 50% of strains encode *nanC* [8]. There is a LPXTG cell wall anchoring motif in the C-terminus of NanA and previous report was also able to locate NanA expression on the bacterial surface by immunogold electron microscopy. In addition, a secreted form of NanA has also been proposed by the authors since the bacterial surface proteases are likely to cleave this LPXTG motif to release NanA into extracellular environment [9]. The proposed functions of NanA include removal of terminal sialic acids found on many human glycoconjugates, which leads to unmask receptors for adherence, to modify the surface of bacteria co-inhabiting the same niche, and to provide a nutrient source [10]. NanA was also involved in pneumococcal biofilm formation independently of its enzymatic activity [11]. In addition, clinical observations suggest that the persisting high mortality in pneumococcal pneumonia is often related to dysregulated hyper-inflammation despite the successful bacterial eradication by antibiotics treatment [12]. An exaggerated pro-inflammatory responses of leukocytes caused by pneumococcal NanA has been reported recently [13]; however, the detailed mechanisms of excess inflammatory response mediated by pneumococcal NanA remain largely unknown.

doi:10.6342/NTU201701774

B. Sialic acid (Sia)-binding immunoglobulin-like lectins (Siglecs)

Siglecs are membrane-bound I-type lectins that constitute Sia-binding immunoglobulin superfamily with distinct cell distribution and glycan specificities [14]. To date, fifteen and nine Siglecs have been identified in humans and mice, respectively (Appendix. Table. S1) [15]. In mammals, there are two subgroups of Siglecs: (i) sialoadhesin (Sn; Siglec-1), CD22 (Siglec-2), MAG (Siglec-4) and Siglec-15, which are expressed in all species; and (ii) CD33-related Siglecs which vary considerably in composition between species and appear to undergo rapid evolution in primates (Appendix. Fig. S1). All Siglecs contain a homologous N-terminal V-set Ig-like domain, which recognizes sialylated glycans, followed by variable numbers of C2- set domains. When expressed on the cell surface, Siglecs interact with Sia-containing ligands both in *cis* (on the same cells) and *trans* (on the different cells). Both types have been shown to play important roles in immune modulation [14,15]. The cytosolic domain of most Siglecs possess two or more immune-receptor tyrosine-based inhibitory motif (ITIM) that can be phosphorylated to create SH2 domain binding sites and recruit SH2 domain-containing effector molecules. It has been reported that enhanced anti-inflammatory IL-10 production and reduced pro-inflammatory TNF-α production upon LPS stimulation can be observed in the Siglec-5 and Siglec-9 overexpressing murine macrophages [16]. Moreover, mutation in the intracellular ITIM motif and essential arginine in the Sia-binding pocket both abolished the Siglec-9-mediated IL-10 production [16,17], which indicates that both the ITIM motif and the lectin activity are critical and essential for the inhibitory immunomodulation of Siglecs. Phosphorylated ITIMs create the docking sites for tandem SH2 domain-containing protein tyrosine phosphatases (SHP)-1 and SHP-2 [15,18,19] . Macrophages from *motheaten* (SHP-1-deficient) mice are hyper-responsive to hematopoietic cell growth factors and other stimuli [20]. In contrast, overexpression of SHP-1 or SHP-2 inhibit Toll-like receptor (TLR) ligand-triggered cytokine production [21,22]. Activating Siglecs, such as Siglec-14 and Siglce-16, are able to associate with DNAX activation protein of 12 kDa (DAP12), an adaptor protein with immune-receptor tyrosine-based activation motif (ITAM); therefore, these Siglecs are suggested to directly trigger signal transduction via Syk recruitment and result in cell activation (Appendix. Fig. S2).

Siglecs are involved in immune-modulation in several aspects. *Cd22*$^{-/-}$ B cells exhibit hyper-activation in response to several TLRs ligands; while the expression of CD22 reduces lipopolysaccharide (LPS)-triggered NF-κB activation *in vitro* [23]. Both

doi:10.6342/NTU201701774

Sigelc-7 and Sigelc-9 can negatively modulate TCR activation, such as de-phosphorylation of ZAP-70 by recruitment of SHP-1, resulting in the reduction of NAFT (nuclear factor of activated T cells)-mediated gene transcriptions [24]. The interaction of CD14 with CD33 regulates its presentation of LPS from CD14 to TLR-4, and eventually results in the attenuated TLR-4-mediated signaling [25]. Furthermore, MyD88-dependent up-regulation of Siglec-E negatively modulates TLR-induced amplification of IFN-β via SHP-2 recruitment [26]. In a model of LPS-induced lung inflammation, Sigelc-E deficient mice showed exaggerated CD11b-dependent neutrophil influx into lung tissue [27]. All these cases point out the significance of Siglecs as an negative regulator in host immunity.

C. Siglec-5 and Siglec-14 paired receptors and their roles in immunity

Due to ongoing gene conversion, the *SIGLEC5* and *SIGLEC14* gene is adjacent to each other on chromosome 19, which encodes proteins 100% identical in their V-set domain and differs in only one amino acid in the first C2 domain. However, they transmit opposite intracellular signals upon ligand engagement. Siglec-5 has an intracellular ITIM motifs to transduce inhibitory signals, whereas Siglec-14 is associated with DAP12 to mediate activating signaling. Both Siglec-5 and Siglec-14 bind similar ligands, with a preference for the sialyl-Tn structure (Neu5Acα2-6GalNAcα) [28]. It has been shown that Siglec-5 is expressed on neutrophils, monocytes and B cells, while Siglec-14 is found at low level on neutrophil and monocytes. A *SIGLEC14* null allele discovered recently is preferentially present in Asian populations but is less common in Europeans [29]. It is generated by a recombination event between the 5' region of the *SIGLEC14* gene and 3' region of the *SIGLEC5* gene, resulting in fusion protein that is identical to Siglec-5 but expressed in Siglec-14 like manner.

Individuals who are *SIGLEC14* null exhibited reduced exacerbation in chronic obstructive pulmonary disease (COPD), when compared with individuals expressing *SIGLEC14* wild-type [29]. It has been demonstrated that both Siglec-5 and Siglec-14 can bind sialylated strains of *Haemophilus influenza* (*H. influenzae*), which is a major cause of COPD exacerbation and binding of Siglec-5 and Siglec-14 with sialylated *H. influenzae* triggered inhibitory and activating responses, respectively. Thereby, the absence of Siglec-14 on myeloid cells would lead to reduced inflammatory responses in *SIGLEC14*-null individuals. Besides expression on leukocytes, both Siglec-5 and Siglec-14 are found on human amniotic epithelium and may influence the host responses to group B *Streptococcus* (GBS) infection and the frequency of preterm births

doi:10.6342/NTU201701774

in infected mothers [30]. Aside from mediating sialic acid-dependent interactions between host cells and pathogens, Siglec-5 and Siglec-14 are capable of mediating Sia-independent interactions with some GBS strains via recognition of bacterial surface β-protein [30]. A recent study also demonstrated that a non-glycosylated danger-associated molecular pattern (DAMP) protein , heat shock protein 70, can modulate cellular responses via direct binding to Siglec-5 and Siglec-14 [31].

D. Cell surface receptors synergize to cellular responses

There are several kinds of receptors resides on cell membrane which act as sensing molecules to deliver signaling and maintain the normal biological functions in dynamic equilibrium. In some cases, these receptors tend to collaborate with each other to make more efficient and correct responses to their corresponding stimuli, including self and non-self molecules. The combined activation of these receptors can result in complementary, synergistic or antagonistic effects through controlling the fine-balanced intracellular responses that modulate innate and adaptive immunity. Co-engagement of FcγRIIB (low affinity immunoglobulin gamma Fc region receptor II-b) to an ITAM-bearing receptor leads to tyrosine phosphorylation of the ITIM by Lyn kinase, recruitment of SHIP, and inhibition of ITAM-induced calcium mobilization and cellular proliferation in B cells [32,33]. It has been shown that clustering of complement receptor 3 and Dectin-1 on lipid raft exerts their coordinated action of TNF-α and IL-6 production upon fungal infection [34]. The association between CD24 with Siglec-10 in human or Siglec-G in mice allows the host cells to discriminate PAMPs from DAMPs by selective repression of the host response to DAMPs [35,36]. Disruption of the CD24-Siglec-G/10 interaction caused by microbial sialidase facilitates the exacerbated virulence-mediated cytokine storm during sepsis [37]. In addition, a broad and direct interaction between Siglecs and TLRs are demonstrated in a recent study [38].

E. Hypothesis

An exaggerated pro-inflammatory responses of leukocytes caused by pneumococcal NanA has been reported recently [13]; however, the molecular mechanisms of how excess inflammatory cytokine response mediated by pneumococcal NanA remain largely unidentified. Besides, several reports demonstrated that Siglecs are important negative regulator in immune-modulation via synergistic coordination with other surface receptors [25,37]. Based on these observations, we hypothesize that during pneumococcal infection, bacterial sialidase may disrupt the Sia *cis*-interaction between Siglecs with other pattern recognition receptors, such as TLRs and results in cellular

doi:10.6342/NTU201701774

activation, followed by excess production of pro-inflammatory substances. In addition, expression of inhibitory Siglec-5 or activating Siglec-14 may influence host cellular responses during pneumococcal NanA-mediated desialylation among different *SIGLEC14* genotypes individuals.

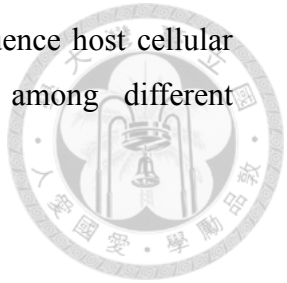

doi:10.6342/NTU201701774

II. Materials and methods

1. Materials

A. Cell lines and culture conditions

Cell lines	Growth conditions	Sources
THP-1 (human acute monocytic leukemia cell line)	37°C with 5% CO_2 in RPMI medium with 10% FBS, 10mM HEPES, 1mM sodium pyruvate, 2.5g/L glucose, 0.05mM 2-ME	American Type Culture Collection (ATCC)
EV/THP-1 (pMSCV-IRES-EGFP transfected in THP-1)	37°C with 5% CO_2 in RPMI medium with 10% FBS	Gift from Dr. Takashi Angata (Academia Sinica)
Siglec-5/THP-1 (pMSCV-IRES-EGFP-Siglec-5 in THP-1)	37°C with 5% CO_2 in RPMI medium with 10% FBS	Gift from Dr. Takashi Angata (Academia Sinica)
Siglec-14/THP-1 (pMSCV-IRES-EGFP-Siglec-14 in THP-1)	37°C with 5% CO_2 in RPMI medium with 10% FBS	Gift from Dr. Takashi Angata (Academia Sinica)

B. Bacterial strains and culture conditions

Bacterial strains	Growth conditions	Sources
S. pneumoniae serotype 2 D39	37°C with 5% CO_2 in THY medium	Gift from Dr. Victor Nizet (UCSD)
S. pneumoniae nanA mutant	37°C with 5% CO_2 in THY medium	Gift from Dr. Victor Nizet (UCSD)

C. Antibiotics

Antibiotics	Stock concentration	Working concentration
Penicillin Streptomycin solution	100X	1X
Puromycin	10 mg/ml	50 μg/ml
Gentamycin	50 mg/ml	100 μg/ml

D. Antibodies

Name	Conjugation	Clone	Source	Application
Mouse IgG1, κ	Nil	MOPC-21	BioLegend	FACS
Human CD170	APC	1A5	BioLegend	FACS
Human CD170	Nil	1A5	BioLegend	IP
Human Siglec-5/Siglec-14	Nil	Goat polyclone	R&D systems	WB
Human CD282 (TLR2)	Nil	TL2.1	BioLegend	IP

doi:10.6342/NTU201701774

Toll-like Receptor 2	Nil	D7G9Z	Cell Signaling	WB
Phospho-NF-κB p65 (Ser536)	Nil	93H1	Cell Signaling	WB
IκB-α	Nil	C-15	Santa Cruz Biotechnology	WB
Phospho-IκB-α (Ser32/36)	Nil	5A5	Cell Signaling	WB
Phospho-Shc (Tyr317)	Nil	Rabbit polyclone	Cell Signaling	WB
SH-PTP1 (SHP-1)	Nil	C-19	Santa Cruz Biotechnology	WB
SH-PTP2 (SHP-2)	Nil	C-18	Santa Cruz Biotechnology	WB
Syk	Nil	N-19	Santa Cruz Biotechnology	WB
Phospho-Syk (Tyr525/526)	Nil	C87C1	Cell Signaling	WB
Flotillin-1	Nil	18/Flotillin1	BD Transduction Laboratories	WB
p38α MAP kinase	Nil	5F11	Cell Signaling	WB
Phospho-p38 MAPK (Thr180/Tyr182)	Nil	D3F9	Cell Signaling	WB
p44/42 MAPK (Erk1/2)	Nil	3A7	Cell Signaling	WB
Phospho-p44/42 MAPK (Erk1/2) (Thr 202/Tyr204)	Nil	D13.14.4E	Cell Signaling	WB
Akt (pan)	Nil	40D4	Cell Signaling	WB
Phospho-Akt (Ser473)	Nil	D9E	Cell Signaling	WB
α-Tubulin 4a	Nil	Rabbit polyclone	GeneTex	WB
β-Actin	Nil	AC-15	Sigma-Aldrich	WB
Donkey α-Mouse IgG	680RD	Polyclone	LI-COR	WB
Donkey α-Rabbit IgG	800CW	Polyclone	LI-COR	WB
Donkey α-Goat IgG	680RD	Polyclone	LI-COR	WB
Streptavidin	800CW		LI-COR	WB
Erythrina Cristagalli Lectin (ECA, ECL)	Biotin		Vector Laboratories	IF
Peanut Agglutinin (PNA)	FITC		Vector Laboratories	FACS

FACS, Fluorescence-activated cell sorting; IP, immuno-precipitation; WB, western blotting; IF, immuno-fluorescent microscopy

doi:10.6342/NTU201701774

E. Antibodies for micro-western array

Name	Regulation	Source
p38α	MAP kinase signaling	Cell Signaling
Phospho-p38 (Thr180/Tyr182)	MAP kinase signaling	Cell Signaling
Phospho-p44/42 MAPK (Erk1/2) (Thr202/Tyr204)	MAP kinase signaling	Cell Signaling
Phospho-Jun(-c) (Ser63)	MAP kinase signaling	Cell Signaling
Phospho-JNK (Thr183/Tyr185, Thr221/Tyr223)	MAP kinase signaling	Millipore
Phospho-MEK1 (Ser218/222)/MEK2 (Ser222/226)	MAP kinase signaling	Millipore
Phospho-MKK3 (Ser189)/MKK6 (Ser207)	MAP kinase signaling	Cell Signaling
Phospho-MKK7/SKK4 (Thr275)	MAP kinase signaling	Millipore
Phospho-Akt (Ser473)	PI3K/Akt signaling	Cell Signaling
PTEN	PI3K/Akt signaling	Epitomics
Phospho-PTEN (Thr366/Ser370)	PI3K/Akt signaling	Epitomics
Phospho-GSK3 (Tyr279/Tyr216)	PI3K/Akt signaling	Millipore
Phospho-PDK1 (Ser241)	PI3K/Akt signaling	Cell Signaling
Phospho-eNOS/NOS III (Ser116)	PI3K/Akt signaling	Millipore
Phospho-PLCγ1 (Tyr783)	Ca/cAMP/lipid signaling	Cell Signaling
Phospho-PKCγ (Thr655)	Ca/cAMP/lipid signaling	Millipore
Phospho-PKD (Ser916)	Ca/cAMP/lipid signaling	Millipore
Phospho-PKD2 (Ser876)	Ca/cAMP/lipid signaling	Millipore
Phospho-PKA (Ser96)	Ca/cAMP/lipid signaling	Millipore
Phospho-Lyn (Tyr507)	Lymphocyte signaling	Cell Signaling
Phospho-Lck (Tyr505)	Lymphocyte signaling	Cell Signaling
Phospho-Syk (Tyr525/526)	Lymphocyte signaling	Cell Signaling
Phospho-Syk (Tyr323)	Lymphocyte signaling	Millipore
Hck (C-term)	Lymphocyte signaling	Epitomics
IkappaB-alpha	NF-κB Signaling	Epitomics
Phospho-IκBα (Ser36)	NF-κB Signaling	Epitomics
Phospho-NF-κB p65 (Ser529)	NF-κB Signaling	Epitomics
LC3A/B	Autophagy Signaling	Epitomics
Beclin-1	Autophagy Signaling	Epitomics

doi:10.6342/NTU201701774

Phospho-acetyl CoA carboxylase (Ser79)	Glucose metabolism	Millipore
Phospho-AMPKα (Thr172)	Glucose metabolism	Cell Signaling
GAPDH	Glucose metabolism	Cell Signaling
GRP-78	Glucose metabolism	Millipore
SREBP1	Glucose metabolism	Millipore
Phospho-SHP-2 (Tyr542)	Phosphatase	Epitomics
Phospho-PP2A (Tyr307)	Phosphatase	Epitomics
HDAC1	Chromatin regulation	Millipore
HDAC3	Chromatin regulation	Millipore
HDAC4	Chromatin regulation	Millipore
Tri-Methyl-Histone H3 (Lys27)	Chromatin regulation	Cell Signaling
Phospho-Shc (Tyr317)	ErbB/HER signaling	Cell Signaling
Phospho-Src (Tyr527)	ErbB/HER signaling	Cell Signaling
Phospho-Src (Tyr416)	ErbB/HER signaling	Millipore
Cleaved caspase-3 (Asp175)	Apoptosis	Cell Signaling
Cleaved caspase-9 (Asp330)	Apoptosis	Cell Signaling
Bcl-2	Apoptosis	BD
Caspase-1	Energy metabolism	Cell Signaling
Phospho-Rictor (Thr1135)	mTOR signaling	Cell Signaling
Phospho-mTOR (Ser2481)	mTOR signaling	Cell Signaling
Phospho-Raptor (Ser792)	mTOR signaling	Cell Signaling
HIF1-α	mTOR signaling	GeneTex
Actin	Cytoskeletal signaling	Abcam
Vav3	Cytoskeletal signaling	Millipore
α-tubulin	Cytoskeletal signaling	OriGene
Phospho-p70 S6 kinase (Thr389),	Translational control	Millipore
Phospho-PKR (Thr446)	Translational control	Millipore
SERPINB2	Inflammation & immunology	OriGene
SOCS3	Jak/Stat signaling	OriGene

doi:10.6342/NTU201701774

F. ELISA (enzyme-linked immunosorbent assay) kit

Name	Catalog Number	Source
hTNF-α	88-7346-88	eBioscence

G. Real-time quantitative polymerase chain reaction (qRT-PCR) primers

Primers	Sequences (5'→3')	Target
hHPRT1-F hHPRT1-R	CAAGCTTGCTGGTGAAAAGGAC GTCAAGGGCATATCCTACAACAAA	Hypoxanthine-guanine phosphoribosyltransferase
hHSPCB-F hHSPCB-R	TCTGGGTATCGGAAAGCAAGCC GTGCACTTCCTCAGGCATCTTG	Heat shock protein 90kDa alpha
hTNFα-F hTNFα-R	CCCAGGGACCTCTCTCTAATCA GCTTGAGGGTTTGCTACAACATG	Tumor necrosis factor alpha

2. Methods

A. Analysis of TNF-α mRNA expression in THP-1 cells upon pneumococcal infection

$1x10^6$ ($2x10^6$/ml, 0.5ml/in siliconized 2ml tube) THP-1 cells were infected with WT SPN or Δ*nanA* SPN at MOI of 10 ($2x10^7$/ml, 0.5ml/in siliconized 2ml tube) for 1 hour at 37°C with rotation. Cells were washed with 1ml ice-cold PBS once and resuspended with 1ml of TRizol reagent. mRNA in the TRizol reagent was further purified by Direct-zol™ RNA MiniPrep kit (ZYMO RESEARCH, Cat. R2052) and purified mRNA was subjected to reverse transcription by PrimeScript™ RT reagent Kit (TaKaRa, Cat. R037A) according to the manufacturer's instruction.

The same experiment was also conducted by PMA-activated THP-1 cells. THP-1 cells ($2x10^6$/ml, 0.5ml/well) were seeded in 24-well in the presence of PMA at final concentration of 25 ng/ml overnight. Activated cells were then refreshed with 1ml fresh complete RPMI medium and incubated for additional 2 days before infection.

B. Analysis of TNF-α protein secretion in THP-1 cells upon pneumococcal infection

$2x10^5$ ($2x10^6$/ml, 0.1ml/well) THP-1 cells were infected with WT SPN or Δ*nanA* SPN at MOI of 10 ($2x10^7$/ml, 0.1ml/well). 50μl of 5X penicillin-streptomycin and gentamycin solution were added at 30 min post-infection and infected cells were cultured for additional 2.5 and 5.5 hours. The supernatant was collected to perform cytokine ELISA analysis.

The same experiment was also conducted by PMA-activated THP-1 cells. THP-1 cells ($2x10^6$/ml, 0.1ml/well) were seeded in 24-well in the presence of PMA at

doi:10.6342/NTU201701774

final concentration of 25 ng/ml overnight. Activated cells were refreshed with 200μl fresh complete RPMI medium and incubated for additional 2 days before infection.

C. Measurement of THP-1 surface desialylation upon pneumococcal infection

1. Flow cytometry (FACS) analysis

$1x10^6$ THP-1 cells ($2x10^6$/ml, 0.5ml/in 2ml siliconized tube) were infected with WT SPN or Δ*nanA* SPN at MOI of 10 or 30 ($2x10^7$/ml or $6x10^7$/ml, 0.5ml/ in 2ml siliconized tube) at 37°C for 3 hour. Cells were washed with 1ml ice-cold PBS and stained with 50μl of FITC-conjugated PNA (50μl of 1:500 diluted FITC-conjugated PNA in FACS buffer) for 20 min at 4°C. After washing with 200μl of PBS twice, cells were resuspended in 500μl FACS buffer and analyzed by flow cytometer.

2. Immuno-fluorescence staining

$4x10^5$ ($8x10^5$/ml, 0.5ml/well) THP-1 cells were seeded on poly-L-lysine coated coverslip in 24-well in the presence of PMA at final concentration of 25 ng/ml overnight. The activated cells were refreshed with 1ml fresh complete RPMI medium and incubated for additional 2 days. Cells were then infected with CFSE (Biolegend, Cat. 422701)-labeled WT or Δ*nanA* SPN at MOI of 10 ($8x10^6$/ml, 0.5ml/well) at 37°C for 1 hour. After infection, cells were washed with warm PBS and fixed in 2% paraformaldehyde/PBS for 1 hour at room temperature. After washing with PBS twice, the fixed cells were permeabilized with 0.5% Triton X-100/fix solution for 10 min at room temperature, washed with PBS twice and blocked with 3% BSA/PBS solution for 1 hour at room temperature. Cells were then incubated with biotin-conjugated ECA (500μl biotin-conjugated ECA diluted in blocking solution) for 2 hour at room temperature, washed with PBS twice and stained with Alexa Flour 568-conjugated streptavidin (1:250 dilution in blocking solution) for 1 hour at room temperature. The stained cells were washed with PBS twice, stained with DAPI (1:1000 dilution in blocking solution) for 20 min at room temperature, washed with PBS twice and observed under fluorescent microscope.

D. Sample preparation and validation for Micro-western array (MWA)

1. MWA of THP-1 cells

$6x10^6$ ($1.2x10^7$/ml, 0.5ml/in 2ml siliconized tube) THP-1 cells were infected with WT SPN or Δ*nanA* SPN at MOI of 5 ($6x10^7$/ml, 0.5ml/in 2ml siliconized tube) at 37°C for 20, 40 and 60 min. Cells were washed with 1ml ice-cold PBS once and lysed in 50μl ice-cold 1% NP-40 lysis buffer with 1x protease & phosphatase

doi:10.6342/NTU201701774

inhibitor cocktail (Thermo, #78442). Cell lysate was kept on ice for 20 min and centrifuged at top speed for 15 min at 4°C. The supernatant was collected and stored at -80°C. Protein concentration was measured by Pierce™ BCA Protein Assay kit (Thermo, #23225). MWA was conducted by Core Instrument Center of National Health Research Institutes and blot intensity was analyzed by Image Studio Ver 5.2 software.

2. MWA of primary macrophages

PBMCs were isolated from buffy coat donated by healthy donors. The genotype of *SIGLEC14* was characterized by genomic PCR according to previous report [39].

$3x10^6$ ($3x10^6$/ml, 1ml/well) primary cells were seeded in 6-well overnight. Cells were then infected with WT SPN or Δ*nanA* SPN at MOI of 3 ($9x10^6$/ml, 1ml/well) at 37°C for 30 and 60 min, respectively. Cells were washed with 1ml ice-cold PBS once and lysed in 50μl of ice-cold Mammalian Protein Extraction Reagent (Thermo, #78503) with 1x protease & phosphatase inhibitor cocktail by scraping cells several times. The resulted cell lysate was kept on ice for 20 min, followed by centrifuging at top speed for 15 min at 4°C. The supernatant was collected and stored at -80°C. Protein concentration and quantification were followed the same procedures applied in THP-1 cells.

3. Validation of MWA results by western blotting

Cell lysates (THP-1 cell: 25μg/lane, primary cell: 15μg/lane) were separated on a 12.5% SDS-PAGE (p-Erk, p-p38, p-Akt, p-IκBα) or 10% (NF-κB p-p65, p-Syk, p-Shc) SDS-PAGE and transferred to a PVDF membrane (Immobilon-FL, Cat. IPFL00010) by SEMI-DRY TRANSFER CELL (BIO-RAD). The membrane was blocked with Odyssey Blocking Buffer (1:1 dilution with PBS) at room temperature for 1 hour and probed with 4ml of primary antibody (1:1000 diluted in blocking solution with 0.1% tween-20) at room temperature for 2 hour (or at 4°C overnight). The membrane was washed with 0.1% PBST for 3-5 times (5-10 min each time) and incubated with 5ml of secondary antibody (1:5000 diluted in blocking solution with 0.1% tween-20 and 0.02% SDS) at room temperature for 0.5-1 hour (protect from light). The membrane was washed with 0.1% PBST for 3-5 times (5-10 min each time) and 0.02% SDS/water once for 5 min, and then soaked in PBS before scanning.

doi:10.6342/NTU201701774

E. Cholesterol depletion – methyl-β-cyclodextrin (MβCD) treatment

$1x10^6$ ($1x10^6$/ml, 1ml/well) THP-1 cells were seeded in 12-well in the presence of PMA at final concentration of 25 ng/ml overnight. To deplete surface cholesterol, cells were treated with 5 mM MβCD (SIGMA, Cat. C4555-1G), which diluted in serum-free RPMI medium at 37°C for 20 or 40 min. Cells were then infected with WT SPN or Δ*nanA* SPN at MOI of 10 ($1x10^7$/ml, 1ml/well) at 37°C for 30 or 60 min. The culture supernatant and cells were collected for ELISA assay and qRT-PCR analysis, respectively.

F. Lipid raft isolation – sucrose gradient ultra-centrifugation

1. Sample preparation

$5x10^7$ ($1x10^8$/ml, 0.5ml/in 2ml siliconized tube) THP-1 cells were infected with WT SPN or Δ*nanA* SPN at MOI of 5 ($5x10^8$/ml, 0.5ml/ in 2ml siliconized tube) for 1 hour at 37°C. Cells were washed with 1ml ice-cold PBS once and lysed in 375μl ice-cold 1% Brij-58/TNE buffer (25mM Tris, 150mM NaCl and 5mM EDTA, pH7.5) containing 1x protease & phosphatase inhibitor cocktail by gently pipetting (do not vortex). The cell lysate was kept on ice for at least 30 min and raft-containing supernatant was collected after centrifuging the cell lysate at 300g at 4°C for 5 min.

2. Lipid raft isolation by sucrose gradient centrifugation

375μl of 80% sucrose/TNE buffer was mixed thoroughly with the protein sample prepared as above description. The mixed solution was transferred into the bottom of a centrifuge tube (BECKMAN, Cat. 331372), and then sequentially overlaid with 6ml of 30% sucrose/TNE and 3.5ml of 5% sucrose/TNE on top of it (sucrose solution must add gently through the tube wall). Finally, mineral oil was added as balancing reagent (range of allowable error should be less than 0.001g). The sucrose gradient samples were spun at 40,000 rpm in a SW-41 rotor for 18 hour at 4°C with slow acceleration and no brake. 700μl solution was collected from the top of the centrifuge tube, resulting in total 14 fractions for each sample. Flotillin-1 was used as lipid raft maker for western blot analysis.

G. Immunoprecipitiation and immunoblotting

$1x10^7$ ($2x10^7$/ml, 0.5ml/in 2ml siliconized tube) Siglec-5 overexpressing THP-1 cells were infected with WT SPN or Δ*nanA* SPN at MOI of 10 ($2x10^8$/ml, 0.5ml/ in 2ml siliconized tube) for indicated time points. Cells were washed with 1ml ice-cold PBS once and lysed in 500μl ice-cold 1% NP-40 lysis buffer with 1x protease

doi:10.6342/NTU201701774

& phosphatase inhibitor cocktail. Cell lysates were pre-cleared with 20μl protein A/G mix magnetic beads (Millipore, Cat. LSKMAGAG02) at 4°C for 2 hour, and then immunoprecipitated with 2μg corresponding antibody for 2 hour followed by addition of 25μl protein A/G magnetic beads and incubating overnight. Immunoprecipitates were washed twice with 0.2% NP-40 lysis buffer with 1x protease & phosphatase inhibitor cocktail and re-suspended in 2x SDS sample buffer for western blot analysis.

H. Examination of direct interaction between pneumococcus and recombinant Siglec-5 or Siglec-14

$1x10^8$ c.f.u. of SPN or group B *Streptococcus* (GBS) A909 strain were incubated with 0.25% trypsin for 30 min at 37°C or 5mU/ml neuraminidase (in 50mM sodium acetate, pH5.8) for 1 hour at 37°C. The treated bacteria were washed with PBS and incubated with 2μg of recombinant Siglec-5.Fc, Siglec-14.Fc (provided by Dr. Takashi Angata) or human IgG in 50μl PBS for 20 min at 37°C. Cells were then stained with biotin-conjugated α-hIgG antibody for 20 min at RT, washed with PBS and stained with APC-conjugated streptavidin (1:500 dilution). Cells were washed with PBS twice and resuspended in 1ml PBS and analyzed by flow cytometer. The selected region (R2) was determined as positively stained population.

I. Statistics

Statistical analysis of all experiments in this study were performed using GraphPad Prism 6 (GraphPad Software, La Jolla, CA). The comparisons between multiple groups were analyzed with one-way ANOVA followed by Tukey post-test or Bonferroni post-test (specified in the figure legends). The comparisons between two groups were analyzed by two-tailed *t*-test. Differences were considered significant at a P value <0.05.

doi:10.6342/NTU201701774

III. Results

A. Pneumococcal sialidase (NanA) mediates cell surface desialylation and leads to enhanced cytokine production

Glycans decorating on the cell surface play a vital role in modulating cell-cell and ligand-receptor interactions in several aspects [40]. Pneumococcal NanA has been shown to cleave terminal Sias of the glycoconjugates on the human airway epithelial cells, which facilitates pneumococcal epithelial adherence [10]. To further examine whether NanA-mediated surface desialylation can also be observed on host innate immune cells, human monocytic THP-1 cells were infected with wild-type (WT) *Streptococcus pneumoniae* (SPN) or isogenic sialidase-deficient mutant (ΔnanA), followed by *Peanut Agglutinin* lectin (PNA) staining to reveal the underlying galactose after surface desialylation. WT SPN-infected THP-1 cells showed the increasing binding of PNA in response to the increased multiplicity of infection (MOI) of SPN; while the same phenomenon could not be observed in ΔnanA-infected THP-1 cells (Fig. 1A). Consistent with the results shown above, WT SPN but not ΔnanA mutant-infected THP-1 cells showed increased level of surface desialylation upon infection when observed under fluorescent microscope. In addition, distinct difference of NanA-mediated local surface desialylation pattern of THP-1 cells infected with WT and ΔnanA mutant was observed (arrowheads in Fig. 1B), whereas WT SPN infection induced pronounced local desialylation of infected cells while ΔnanA mutant does not.

To further investigate whether NanA-mediated desialylation of surface glycoconjugates may modulate innate immune responses upon pneumococcal infection, human THP-1 cells were infected with WT SPN and ΔnanA mutant, followed by analyzing the TNF-α production, a prominent pro-inflammatory cytokine massively produced in an acute bacterial infection. As shown in Fig. 2, THP-1 cells infected with WT SPN triggered stronger TNF-α expression compared to cells infected with ΔnanA mutant, in both mRNA (Fig. 2A) and protein level (Fig. 2B). Similar responses were also observed in the PMA-differentiated THP-1 macrophages (Fig. 2C and 2D). Our observations support the general assumption that surface Sia-containing glycoconjugates function as *cis*-ligands to suppress the cell activation through engaging cognate Siglec receptors in the same cells.

B. Lipid rafts are required for NanA-mediated TNF-α exacerbation

Lipid rafts which are micro domains highly enriched with cholesterols,

doi:10.6342/NTU201701774

glycosphingolipids, and various signaling receptors and molecules that play important roles in initiation and transduction of the signaling cascade upon ligand stimulation [41]. Ligand-specific TLR-4 clustering and signaling in lipid rafts following LPS stimulation of monocytes has been reported previously [42]. On the other hand, signal transductions delivered by receptors on lipid rafts would be interfered by the depletion of cholesterols by chemical agent, such as methyl-β-cyclodextrin (MβCD) [34,43]. To test whether clustering of signaling molecules in the lipid raft may be involved in NanA-potentiated TNF-α production upon pneumococcal infection, we compared the TNF-α production from MβCD-pretreated THP-1 cells infected with WT SPN or ΔnanA mutant, respectively. Depletion of cholesterols from lipid rafts partially abrogated NanA-potentiated TNF-α production in both mRNA (Fig. 3A) and protein levels (Fig. 3B), suggesting that lipid rafts possibly contribute to orchestrate signal cascades involving in pneumococcal NanA-regulated signaling cascade.

C. Pneumococcal NanA dysregulates the recruitment of TLR-2 to lipid raft in parental THP-1 cells

Lipid rafts have been reported to both positively and negatively regulate downstream signaling cascade through controlling the physical recruitment or sequestration of the involved signaling molecules [41]. It has been shown that the localization of TLR-2 and Siglec-9 on lipid raft partly modulates IL-10 production [16,17]. We therefore addressed whether surface desialylation by NanA modulates the lipid raft formation or signaling molecule clustering in the lipid raft. Lysates of uninfected THP-1 cells or SPN-infected THP-1 cells were subjected to sucrose gradient centrifugation to isolate the raft and cytosol fractions, and successful separation of the lipid rafts from the cytosol fractions were clearly demonstrated by detection with western blot using specific antibody recognizing flotillin-1 (raft marker shown in Fig. 4A) and α-tubulin (cytosol marker shown in Fig. 4B). In addition, THP-1 cells infected with WT SPN showed moderately increased amount of rafts in the isolated fraction 4 to 7, compared to fractions isolated from uninfected cells and ΔnanA mutant-infected cells.

Data shown in Fig. 3 suggest that lipid rafts are possibly involved in orchestrating NanA-modulated signaling cascade. We then further investigated whether surface desialylation affects the recruitment of TLR-2 and Siglec-5, endogenously expressed by THP-1 cells, to the rafts. Raft fractions (fraction 4, 5, 6, 7) isolated from THP-1 cells infected with WT SPN or ΔnanA mutant were probed with antibody recognizing TLR-2 and Siglec-5, respectively. Our result showed that increased TLR-2 (Fig. 4C) can be

doi:10.6342/NTU201701774

detected in the raft fractions upon WT SPN infection; however, we failed to detect the Siglec-5 signal in the same fraction due to low endogenous level of Siglec-5 expression in the parental THP-1 cells. To compensate limitation mentioned above, THP-1 cells overexpressing Siglec-5 (Sig5/THP-1) were used instead of parental THP-1 cells to address the same question. Lysates of uninfected Sig5/THP-1 cells or SPN-infected Sig5/THP-1 cells were subjected to sucrose gradient centrifugation to isolate the raft fractions, and successful separation of the lipid rafts were demonstrated by detection with western blot using specific antibody recognizing flotillin-1. In contrary to the uninfected control only showing a major flotillin-1 signal in fraction 4 (Fig. 5A), infection of Sig5/THP-1 cells by WT and ΔnanA SPN both resulted in the redistribution of flotillin-1 signal into fraction 4 and 5 (Fig. 5B and 5C). In addition, TLR-2 and Siglec-5 were also redistributed into both fraction 4 and 5 upon SPN infection when comparing to the uninfected control which showing detectable signals for TLR-2 and Siglec-5 in the fraction 5 and 6 (Fig. 5). Taken together, differential distribution of raft marker (flotillin-1), TLR-2 and Siglec-5 upon SPN infection may suggest that the content or the size of lipid rafts can be altered after infection, which later on may affect downstream signal crosstalk of TLR-2 and Siglec-5.

It has been reported that SHP-1, uniquely expressed in hematopoietic system, and SHP-2, ubiquitously expressed in various human tissues, distinctively modulate signaling cascade and immune activation by dephosphorylating their specific substrates [44-46]. We therefore wanted to further explore whether surface desialylation not only affects the recruitment of surface receptors but also regulate the recruitment of SHP-1 and SHP-2 to lipid rafts upon SPN infection. Notably, although the distribution pattern of SHP-1 and SHP-2 were similar in uninfected or SPN-infected Sig5/THP-1 cells (Fig. 5A-C), SHP-1 seemed to reside on raft-associated fractions (fraction 4-6), while SHP-2 was largely excluded from raft fractions.

D. Interrupted interaction between TLR-2 and Siglec-5 and dissociation of SHP-1 from Siglec-5 upon pneumococcal NanA-mediated surface desialylation.

Sia *cis*-interaction between cell surface receptors is responsible for controlling cell stability in steady state. We then further investigated whether the removal of terminal Sia from cell surface by pneumococcal NanA disrupts the TLR-Siglec interaction and contributes to exacerbated cytokine production. Cell lysates were subjected to TLR-2 immunoprecipitation after WT or ΔnanA SPN infection, then probed with PNA and Siglec-5, respectively. The increased PNA and decreased Siglec-5 signals were

doi:10.6342/NTU201701774

observed in WT SPN-infected Sig5/THP-1 cells when comparing to ΔnanA SPN-infected Sig5/THP-1 cells (Fig. 6A). It suggested that the removal of Sia from TLR-2 by pneumococcal NanA affects its interaction with Siglec-5. To further examine whether interrupted interaction of Siglec-5 from TLR-2 influenced the recruitment of intracellular signaling molecules, cell lysates from WT or ΔnanA SPN infected cells were immunoprecipitated with anti-Siglec-5 antibodies, followed by detection of Siglec-5-associated phosphatases or adaptor Grb2 by specific antibodies recognizing SHP-1, SHP-2 and Grb2. We found a reduced recruitment of phosphatase SHP-1 to Siglec-5 at 40 min in WT SPN-infected cells; while the recruitment of SHP-2 to Siglec-5 was similar between WT and ΔnanA SPN-infected Sig5/THP-1 cells (Fig. 6B). It has been reported that Grb2, an adaptor protein involved in signal transduction, is recruited to phosphorylated tyrosine of CD22 cytoplasmic tail in B cell during BCR crosslinking [47,48]. In addition to the reduced recruitment of hematopoietic SHP-1 to Siglec-5, a transient but robust recruitment of Grb2 to Siglec-5 was also observed in WT SPN-infected Sig5/THP-1 cells (Fig. 6B). In summary, our data suggest that diminished interaction between inhibitory Siglec-5 and TLR-2 upon pneumococcal NanA-mediated surface desialylation may lead to enhanced recruitment of Grb2 and reduced association with SHP-1, which contributes to the exacerbated inflammation upon SPN infection.

E. Systematic identification of signaling molecules involved in pneumococcal NanA-provoked cytokine production by Micro-Western Array

To broadly search for the undisclosed mechanisms involved in pneumococcal NanA-mediated exacerbated inflammation, micro-western array (MWA) was applied to probe for selected phospho- and non-phospho-proteins, which are involved in signal transduction. Signal intensity revealed by 31 out of 48 antibodies used for MWA with correct protein molecular weight was summarized in Fig. 7. Candidates identified by MWA were further validated by regular western blot analysis (Fig. 8). In accordance with MWA data, the phosphorylation of Shc and Syk (20 min post-infection), as well as Erk, p38, Akt, IκBα and p65 subunit of NF-κB (60 min post-infection) were augmented by pneumococcal NanA. Taken together, our data showed that pneumococcal NanA potentiates the activation of Shc, Syk, as well as important molecules involved in the PI3K/Akt, NF-κB and MAPK pathways.

F. *SIGLEC5/14* gene polymorphism influences human primary macrophage responses upon pneumococcal NanA-mediated surface desialylation

doi:10.6342/NTU201701774

Siglec-5 and Siglec-14 are paired receptors, sharing a high degree of amino acid sequence identity in their extracellular region, with the two outermost Ig-like domain being 99% identical [28,39]. In previous studies, group B *Streptococcus* (GBS) has been shown to generate opposite immune responses through directly engaging inhibitory Siglec-5 or activating Siglec-14 receptor via bacterial β-protein [30]. Inspired from these observations, we hypothesized that bacterial neuraminidase-mediated host desialylation which disrupts the *cis*-interaction between Siglecs with their surface ligands may drive distinct immune responses through Siglec-5 and Siglec-14. To address this hypothesis, human primary macrophages with indicated genotypes were infected with WT SPN or ΔnanA mutant, and the secretion of inflammatory cytokine was examined at indicated time point. In accordance with previous observations (Fig. 2) on THP-1 cells which only express Siglec-5 and lack detectable Siglec-14 expression, exaggerated TNF-α secretion was detected on WT SPN-infected Siglec-$14^{-/-}$ primary macrophages, when comparing to ΔnanA-infected cells (Fig. 9A). Surprisingly, ΔnanA but not WT SPN stimulated stronger TNF-α secretion on Siglec-$14^{+/+}$ primary macrophages (Fig. 9B). To rule out the possibility that above observations are caused by direct engagement of Siglecs by pneumococcal surface molecules, WT SPN was stained with recombinant Siglec-14.Fc, Siglec-5.Fc or human IgG and examined by FACS analysis. We found that neither Siglec-14 nor Siglec-5 directly interacts with WT SPN (Fig. 10A-C). GBS A909 strains here served as positive staining control, since the interaction between GBS β-protein and Siglec-5 and Siglec-14 has been well documented (Fig. 10D-F). Taken together, Siglec-$14^{+/+}$ primary macrophages lost the tendency to induce aggravated TNF-α secretion induced by NanA-mediated desialylation.

G. TNF-α secretion from Siglec-5 and Siglec-14 overexpressing THP-1 cells upon pneumococcal infection

To ascertain whether expression of Siglec-5 and Siglec-14 is critical and essential for the differed TNF-α production pattern we observed on the primary macrophages isolated from Siglec-$14^{-/-}$ and Siglec-$14^{+/+}$ individuals, THP-1 cells overexpressing only Siglec-5 (Sig5/THP1) or Siglec-14 (Sig14/THP1) were infected with WT SPN and ΔnanA mutant to examine their TNF-α production. In concordance with previous observations on parental THP-1 cells and primary Siglec-$14^{-/-}$ macrophages, WT SPN, comparing to ΔnanA mutant, induced excess TNF-α secretion at MOI of 30 in both EV/THP1 and Sig5/THP1 cells. However, this differed TNF-α secretion upon WT SPN and ΔnanA mutant infection cannot be observed in Sig14/THP1 cells (Fig. 11) in which

doi:10.6342/NTU201701774

WT SPN and ΔnanA mutant induced similar TNF-α secretion. Notably, the TNF-α production in the uninfected Sig-14/THP-1cells were higher than uninfected EV/THP1 and Sig5/THP1, which may result from the reduced cell activation threshold when overexpressing an activating receptor, Siglec-14.

To test whether expressing an activating receptor, Siglec-14 reduced cell activation threshold, we examined the Erk phosphorylation of primary macrophages derived from defined Siglec-5/-14 genotype upon pneumococcal infection. WT SPN infection triggered an increased Erk phosphorylation in the macrophages both from Siglec-$14^{+/+}$ and Siglec-$14^{-/-}$ individuals, however, Siglec-$14^{+/+}$ macrophages showed a high basal level of Erk phosphorylation prior to SPN infection and a delayed kinetic of Erk activation upon SPN infection (Fig. 12A and 12C). An increased Erk phosphorylation also can be observed in the primary macrophages derived from Siglec-14 heterozygote individuals upon WT SPN infection when comparing to cells infected ΔnanA mutant, although the difference was gone 60 min post-infection (Fig. 12B).

H. Systematic identification of signaling molecules differed in Siglec5/14 genotype upon pneumococcal infection

To screen the signaling cascade differed in Siglec-5/-14 paired receptors upon pneumococcal NanA-mediated desialylation, MWA was applied to probe for selected phospho- and non-phospho-proteins, which are involved in signal transduction. Signal intensity revealed by 31 out of 48 antibodies used for MWA with correct protein molecular weight were summarized for all three different Siglec-5/-14 genotype combination (Fig. 13A) or only for Siglec-$14^{+/+}$ individual (Fig. 13B). The universal hyper-phosphorylation was observed in Siglec-$14^{+/+}$ individual compared with Siglec-$14^{-/-}$ individual. To our surprise, WT SPN still provoked stronger activation of MAPK and PI3K/Akt pathways in Siglec-$14^{+/+}$ individuals, which was similar to what we found in Siglec-$14^{-/-}$ individuals. It suggested that other signaling pathways but not MAPK and PI3K/Akt pathways are involved in the distinct TNF-α secretion pattern observed in the Siglec-$14^{+/+}$ and Siglec-$14^{-/-}$ individuals.

I. Examine the expression of Ezh2 and histone3 Lys27 trimethylation in *SIGLEC14* WT and null individuals upon pneumococcal infection

Intriguingly, from the results of MWA, we found that an opposite regulation of histone3 Lys27 trimethylation (H3K27-me3) in *SIGLEC14* WT and null individuals upon WT and ΔnanA SPN infection. H3K27-me3 is considered as a marker for

doi:10.6342/NTU201701774

transcriptional switch off. Increased level of H3K27-me3 might be one of the explanation for the attenuated cytokine production observed in *SIGLEC14* WT individuals upon WT SPN infection. Ezh2 is the catalytic subunit of histone methyl transferase complex-PRC2 (polycomb repressive complex 2) and specifically add methyl group on histone3 Lys27. We then further examined the expression of Ezh2 and H3K27-me3 in primary macrophages with different *SIGLEC14* genotype upon WT and ΔnanA SPN infection. WT SPN infection exhibited higher degree of H3K27-me3 at 60 min compared to ΔnanA SPN infection in Siglec14$^{-/-}$ primary macrophage. However, there was no significant difference in Ezh2 expression upon WT and ΔnanA SPN infection (Fig. 14A). On the other hand, WT SPN infection elicited higher degree of H3K27-me3 at 30 min post infection compared to ΔnanA SPN infection in Siglec14$^{+/+}$ primary macrophages. Unexpectedly, expression of Ezh2 together with H3K27 trimethylation was largely diminished at 60 min after SPN infection, however this phenotype needed to be further confirmed due to limited sample size.

doi:10.6342/NTU201701774

IV. Discussion

In the current study, we demonstrated that pneumococcal NanA-mediated surface desialylation provokes cytokine production by THP-1 cells. Augmented cytokine production mediated by pneumococcal NanA may result from the diminished interaction between Siglec-5 and TLR-2, which leads to reduced recruitment of phosphatase SHP-1 to Siglec-5 to antagonize MAPK, PI3K/Akt and NF-κB signaling pathways (Fig. 15). In addition, *SIGLEC14* polymorphism affects host immune responses upon pneumococcal infection in which NanA has opposite effects in modulation of cytokine production from primary macrophages derived from *SIGLEC14* wild type and null individuals. NanA potentiates inflammatory cytokine production in primary macrophages with homozygous *SIGLEC14* null allele but not macrophages derived from individuals with homozygous *SIGLEC14* wild type allele upon pneumococcal infection. Stronger activation of MAPK and PI3K/Akt pathways can be observed in both macrophages derived from *SIGLEC14* wild type and null individuals upon wild type SPN infection, which suggests that those two general pathways downstream of TLR-2 are not responsible for the differential inflammatory cytokine production observed among the individuals with different *SIGLEC14* genotypes.

Innate immune system plays critical roles in host first-line defense, both in pathogen clearance and host tissue repairs. The normal defensive exertion of host cells heavily relies on exquisite interplay between ligand-receptor recognition and receptor-receptor coordination to provide maximal protection with minimal immunopathology. Pattern recognition receptors (PRR), such as Toll-like receptors (TLRs) or Nod-like receptors (NLRs), are capable to recognize PAMPs (pathogen associated molecular patterns) and/or DAMPs (danger-associated molecular patterns) derived from foreign components and self-molecules, respectively [49,50]. The biological significance of inhibitory roles of Siglecs in TLRs-mediated inflammatory responses has been demonstrated in several previous reports. Compared to *Siglece* WT mice, *Siglece* knockout mice showed augmented TNF-α and IL-6 secretion during *E.coli* infection [51]. LPS-induced TNF-α secretion was inhibited in Siglec-9 overexpressing murine macrophages [16]. A broad and direct interactions between TLRs and Siglecs demonstrated by a recent publication provides a missing link for a potential synergistic coordination in immune-regulation between these two PRRs families [38]. Based on these observations, ITIM-containing Siglecs are thought to be negative regulators to restrain TLRs function and avoid exacerbated cell activation. However, the underlying

doi:10.6342/NTU201701774

mechanisms of how and where ITIM-containing Siglecs deliver downstream signals to suppress TLR signaling and the signaling molecules involved in this inhibitory functions are not fully explored.

Intracellular signaling processes initiated by extracellular stimulation tightly control cellular biological functions. Protein tyrosine phosphatases, which function to dephosphorylate key intermediaries in ligand-receptor signaling pathways, play equally important roles as protein kinase in signal transduction. SHP-1 (Src-homology-2-domain-containing protein tyrosine phosphatase 1) and SHP-2 exhibit distinct functions in immune regulation based on their cell distributions and substrate specificities [44-46,52]. The roles and functions of SHP-1 and SHP-2 in myeloid lineages have not been fully understood until recent decade. In previous studies, the phenomenon that an increased movement of Siglec-9 and SHP-2 to membrane rafts were observed upon PGN (TLR-2 ligand) stimulation in Siglec-9 overexpressing murine macrophages; but the amount of SHP-1 on lipid rafts were not affected [17]. In addition, the inhibitory activities of CD300a, a membrane protein expressed on myeloid lineages and specific subsets of $CD4^+$ T cells, in MyD88 and TRIF-mediated cell activation required SHP-1 and/or SHP-2 in human monocytic cell lines [53]. The above two cases indicated that SHP-1 or SHP-2 is specifically and exclusively recruited to certain ITIM-bearing receptors and exert its inhibitory properties depending on the applied experimental system. Based on membrane fractionation (Fig. 5) and co-immunoprecipitation (Fig. 6B) experiments in our study, SHP-1 is more likely one of the tyrosine phosphatase candidates, which modulates signal transduction upon the interrupted interaction of Siglec-5-TLR-2 by pneumococcal NanA in our infected THP-1 system. However, the role of another ITIM-associated phosphatase SHIP-1 (SH2-containing inositol-5-phosphatase-1) in NanA-mediated desialylation cannot be excluded.

Microbial neuraminidase is well accepted as a virulent factor during their pathogenicity [54,55]. Viral neuraminidase plays essential roles in final stage of infection in which neuraminidase cleaves sialic acids from cell surface and progeny virions facilitate virus release from infected cells [56]. Moreover, a recent study has shown that viral neuraminidase promotes virus access to target site and entry into the cells during early stage of infection [57]. On the other hand, bacterial neuraminidase exerts versatile functions through the whole infection process, including mucus degradation to reduce viscosity from entrapment, host receptor uncovering for adherence and surface modifying of co-inhabiting bacteria for their own survival advantages [10]. In this report,

doi:10.6342/NTU201701774

we demonstrated that pneumococcal NanA also plays critical roles in modulating the activation magnitude of immune cells. We demonstrated that the augmented cytokine production and cell activation observed in the WT pneumococcus infected cells is NanA-dependent by applying the unique SPN isogenic mutant only differing in the NanA expression (ΔnanA mutant) (Fig. 2 and Fig. 8). Intriguingly, a recent report also demonstrated that the expression and localization of host neuraminidase can also be altered upon microbial infection, which also contributes to the host cell desialylation [37]. In addition, the association between Siglec-E and TLR-4 was disrupted via translocation of Neu1 to cell surface which results in enhanced cytokine production upon LPS stimulation [38]. Therefore, the involvement of host neuraminidase in our experimental system may not be ruled out since host Neu1 may also translocates to cell surface to initiate surface desialylation via activation of TLR-2 by Gram-positive pneumococcus upon infection.

Two paired Siglec receptors (Siglec-5 with Siglec-14 and Siglec-11 with Siglec-16) are able to generate opposite immune responses when engaged by bacterial pathogens or host endogenous proteins [15,28,30,58-60]. The activating Siglecs, Siglec-14 and Siglec-16, have been proposed to have evolved to counteract pathogens that subvert host immune surveillance by Sia molecular mimicry through inhibitory Siglec-5 and Siglec-11. We speculate that the converse may be true that bacterial neuraminidase-mediated desialylation can influence host immune responses among different *SIGLEC14* genotypes through removal of the *cis*- ligands. In Siglec-$14^{-/-}$ primary cells, PRRs may form *cis*-interaction with Siglec-5 through Sias and transduce an inhibitory signaling by phosphatase activity, and this hypothesis was supported by the evidence that when SPN infection causes surface desialylation, Siglec-5 no more restrains activating signaling initiated by PRRs and results in exaggerated cytokine production (Fig. 16; left panel). On the other hand, in Siglec-$14^{+/+}$ primary cells, Siglec-14 initiates downstream signal via adaptor protein DAP12 in response to the *cis*-interaction with PRRs, which therefore leads to Syk recruitment and elicits constitutive signaling transduction, followed by a higher level cytokine secretion in steady state. Surface desialylation mediated by pneumococcal NanA may disrupt this *cis*-interaction and result in dissociation of Syk from DAP12 and attenuation of cytokine production. (Fig. 16; right panel).

Based on the results shown in Fig. 9 and Fig. 11, cells with only Siglec-5 or Siglec-14 expression respond differently to infection caused by SPN WT and ΔnanA mutant

doi:10.6342/NTU201701774

both in an *ex vivo* and *in vitro* model systems. In addition, when overexpressing an activating Siglec-14 in THP-1 cells, a higher basal level of TNF-α secretion in steady state could be observed compared to parental THP-1 cells and THP-1 cells overexpressing an inhibitory Siglec-5 (Fig. 11). It suggests that massive expression of an activating receptor on cell surface may reduce the threshold of cell activation and the aggravated responses would be elicited upon induction by extracellular stimuli. To further ascertain this observation in primary cells, $CD14^+$ monocyte-derived macrophages were isolated from individuals with different *SIGLEC14* genotypes and stimulated with LPS. However, as shown in Fig. 17, there is no significant difference of TNF-α secretion between different *SIGLEC14* genotype individuals followed by LPS treatment. In contrary to our observation, Ali et al. previously demonstrated that Siglec-$14^{+/+}$ monocytes tend to have stronger TNF-α secretion compared to Siglec-$14^{-/-}$ monocytes upon LPS stimulation [30]. This conflict may result from the different experimental system in which the expression of Siglec is gradually down-regulated when we differentiated the monocytes into macrophages in the *ex vivo* cultured system. Downregulation of Siglec expression on cell surface may contribute to the similar inflammatory cytokine production upon extracellular stimulation. In the future, we will repeat the same experiment in primary monocyte system.

To dissect the signaling molecules participating in the differed cytokine production observed in primary macrophages from different *SIGLEC14* genotype upon SPN infection, a broad and systematic approach was applied to explore the potential candidates. However, micro-western array (MWA) results showed MAPK, PI3K/Akt signaling pathways are all potentiated by pneumococcal NanA in *SIGLEC14* WT and null individuals, which suggests other signaling molecules are involved in this distinct phenotypes observed in different *SIGLEC14* genotypes upon pneumococcal infection. Intriguingly, the modifications of H3K27-me3, viewed as a marker of transcriptional silencing, showed opposite regulation in primary cells with different *SIGLEC14* genotypes upon SPN infection. The higher level of H3K27-me3 in Siglec-$14^{+/+}$ cells may be one of the explanations of attenuated TNF-α secretion upon NanA-mediated desialylation. Unfortunately, when ascertaining the phenomenon observed in MWA by another paired primary samples, the modification of H3K27-me3 were similarly enhanced by WT SPN infection in both *SIGLEC14* null and WT individuals. The inconsistent outcomes might be due to the individual variations in our limited sample size. In the future, we will use cell lines expressing only Siglec-5 or Siglec-14 to further

doi:10.6342/NTU201701774

examine the level of H3K27-me3 upon SPN infection.

In summary, we tried to elucidate the molecular mechanisms of interplay between Siglec and TLR upon surface desialylation mediated by bacterial sialidase. Our findings may provide potential mechanism for the hyper-inflammation phenotype observed in SPN-infected patients even after successful elimination of pneumococcus by antibiotics. Furthermore, *SIGLEC14* genotypes may alter the outcomes of inflammation upon SPN infection, and the further investigation of the roles of Siglec-5 and Siglec-14 in immune-modulation may provide a new diagnostic predictor for the course of disease progression upon pneumococcal infection.

doi:10.6342/NTU201701774

V. Figures

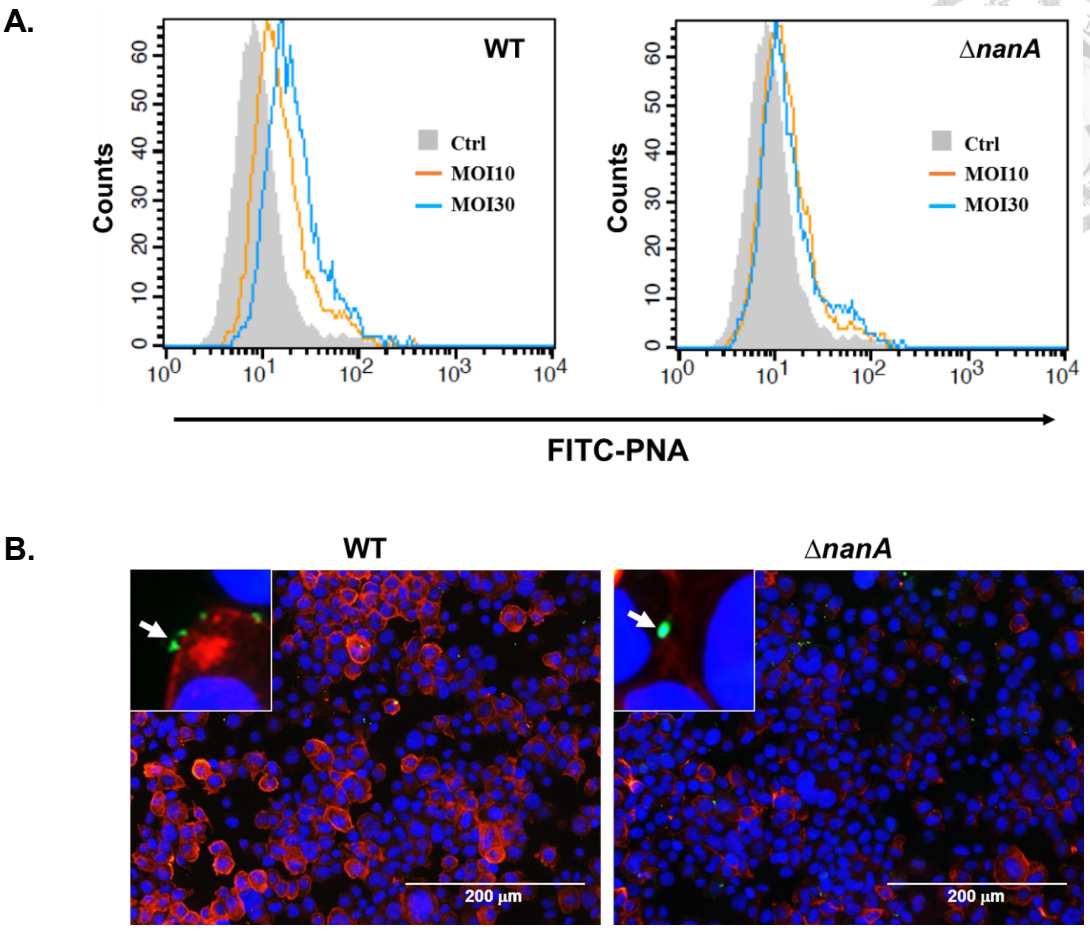

Figure 1. Pneumococcal NanA mediates cell surface desialylation. (A) Cell surface desialylation was determined by FITC-conjugated PNA staining of human THP-1 cells infected with WT or Δ*nanA* SPN at MOI of 30 (blue line) or 10 (orange line), respectively. (B) THP-1 infected with CFSE-labeled WT or Δ*nanA* SPN at MOI of 30 for 1 hour was stained with biotinylated ECA, followed by a secondary Alexa flour 568-conjugated streptavidin and DAPI to visualize exposed galactose (red) and nucleus (blue), respectively. White arrowheads indicate CFSE-labeled bacteria (green). Representative immunofluorescent micrographs are shown from two independent experiments.

doi:10.6342/NTU201701774

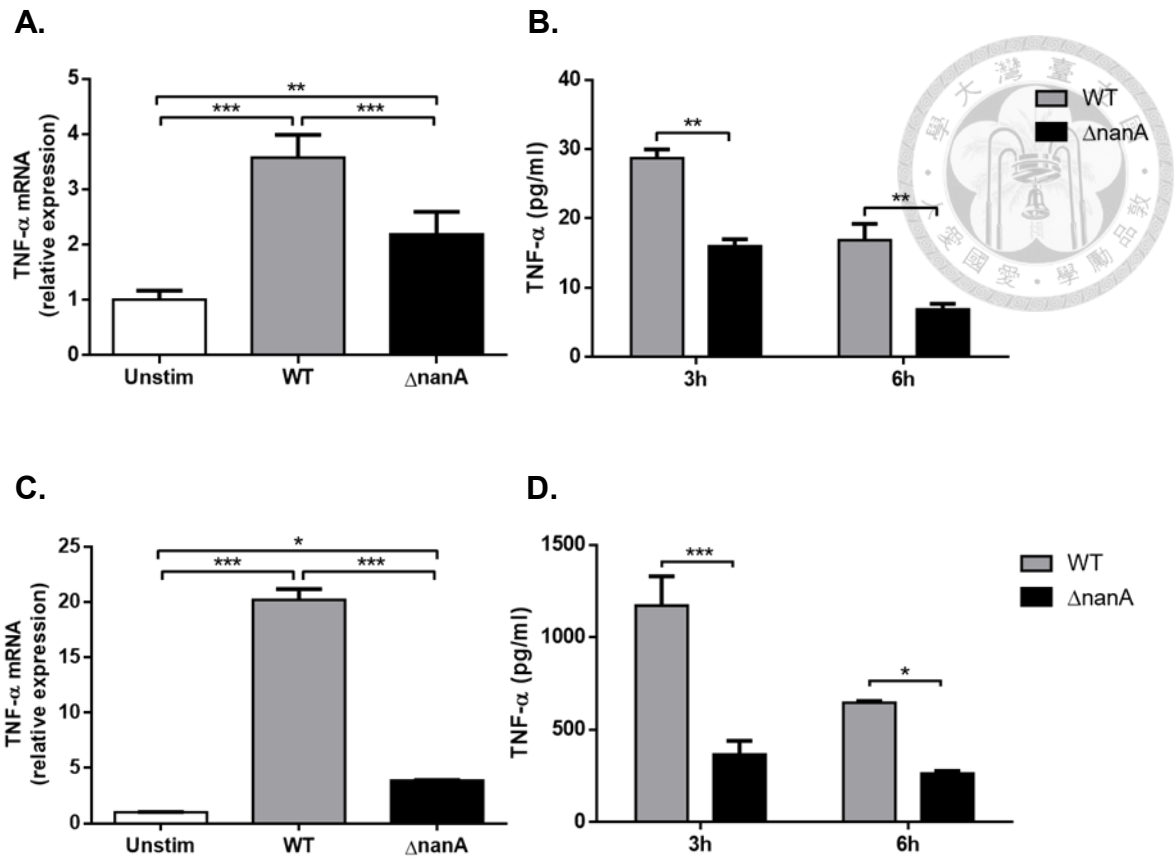

Figure 2. Pneumococcal NanA-mediated surface desialylation leads to enhanced cytokine productions. PMA-activated THP-1 cells were infected with WT or Δ*nanA* SPN at MOI of 10. mRNA was collected at 1 hour p.i. and supernatant was collected at 3 and 6 hour p.i.. mRNA and protein levels of multiple cytokines were quantified by qRT-PCR (A, C, E, G) and ELISA (B, D, F, H), respectively. Data presented are mean ± SEM. Data shown are pooled from two or three independent experiments. Difference between experimental groups are calculated by one way ANOVA with Bonferroni's multiple comparisons test. * $p<0.05$, ** $p<0.01$, *** $p<0.005$.

doi:10.6342/NTU201701774

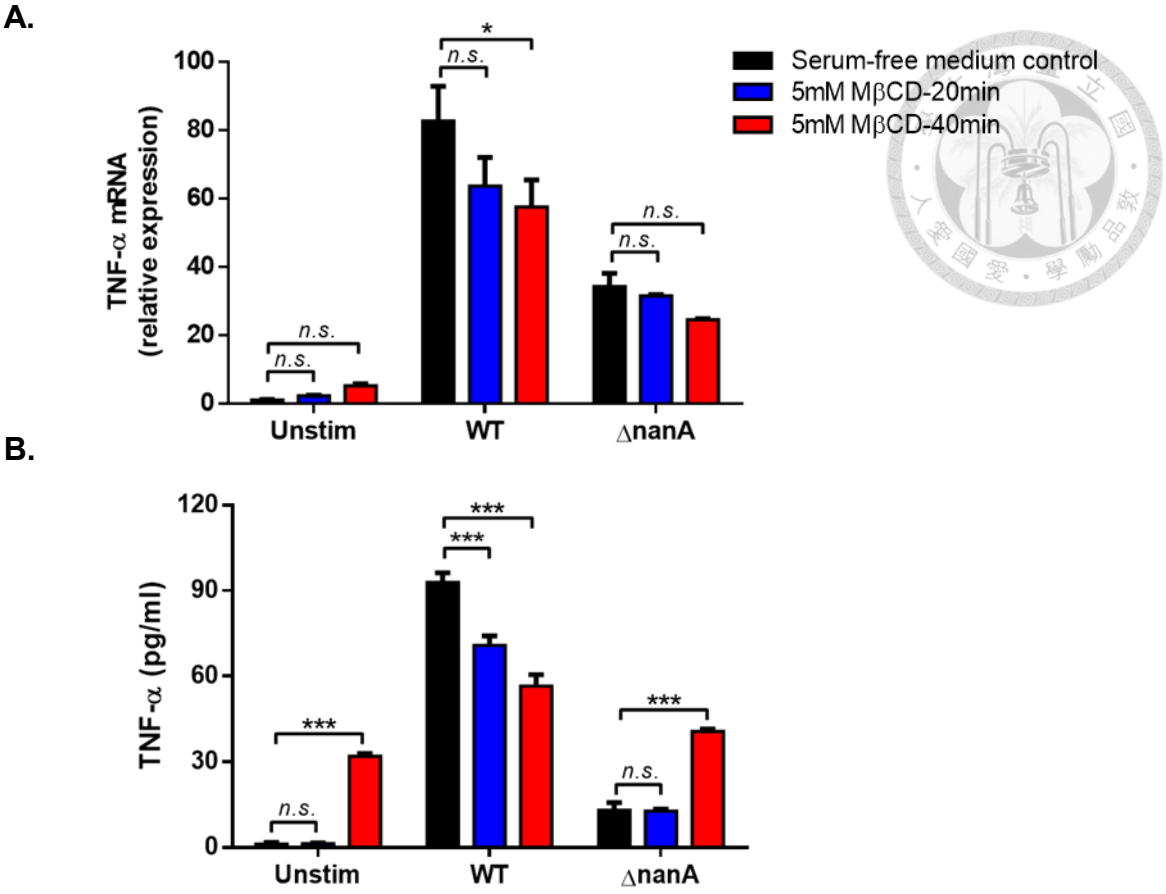

Figure 3. Depletion of lipid raft partially abolishes NanA-mediated TNF-α augmentation. PMA-activated THP-1 cells were pretreated with 5 mM MβCD for 20 and 40 min, respectively, prior to infecting with WT or Δ*nanA* SPN at MOI of 10. Cells and culture supernatant were collected 1 hour p.i. to quantify the TNF-α mRNA (A) and secreted TNF-α cytokine (B), respectively. Data presented are mean ± SEM. Difference between experimental groups are calculated by one way ANOVA with Bonferroni's multiple comparisons test. * $p<0.05$, ** $p<0.01$, *** $p<0.005$. *n.s*, not significant.

doi:10.6342/NTU201701774

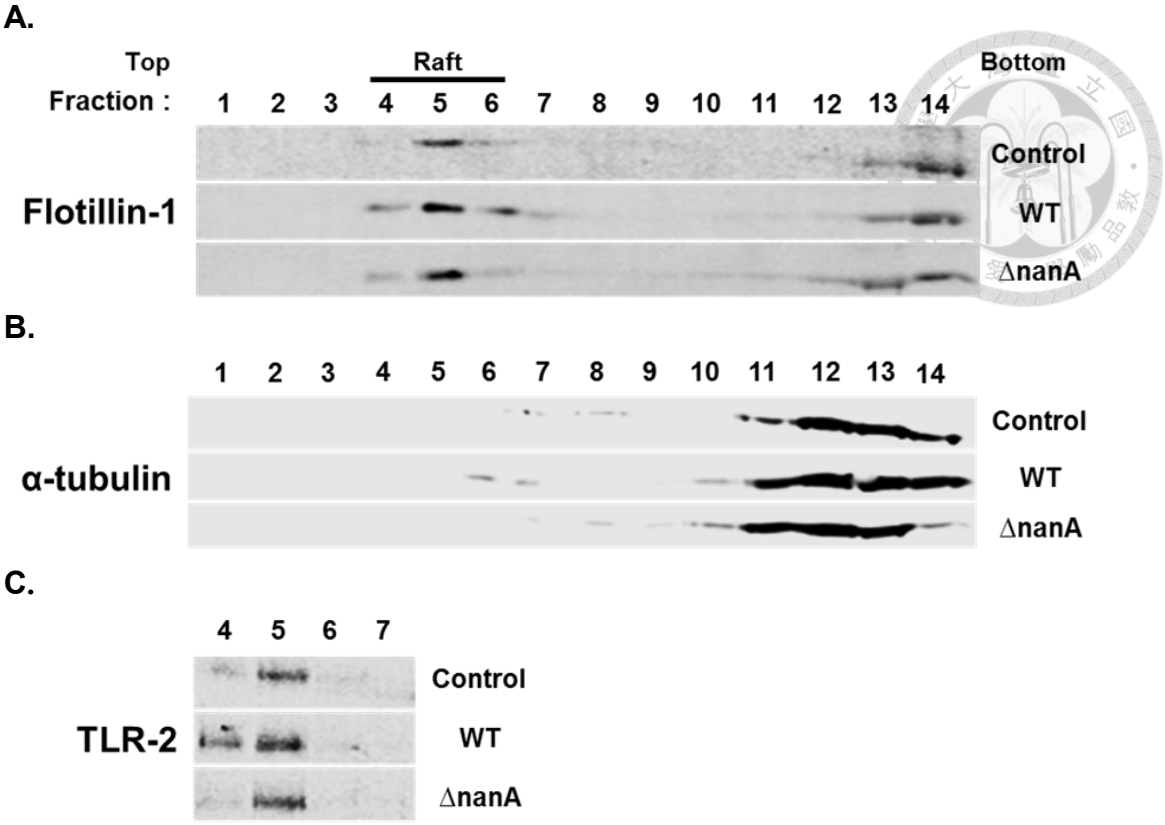

Figure 4. Pneumococcal NanA dysregulates the recruitment of TLR-2 to lipid raft. THP-1 cells were infected with WT or Δ*nanA* SPN at MOI of 5 for 1 hour, followed by sucrose gradient centrifugation to separate raft and cytosol fractions. Successful sucrose fractionation was validated by western blot to probe with flotillin-1 (A) and α-tubulin (B). The distribution of TLR-2 (C) was analyzed on sucrose fraction 4-7. Representative data from two independent experiments are shown.

doi:10.6342/NTU201701774

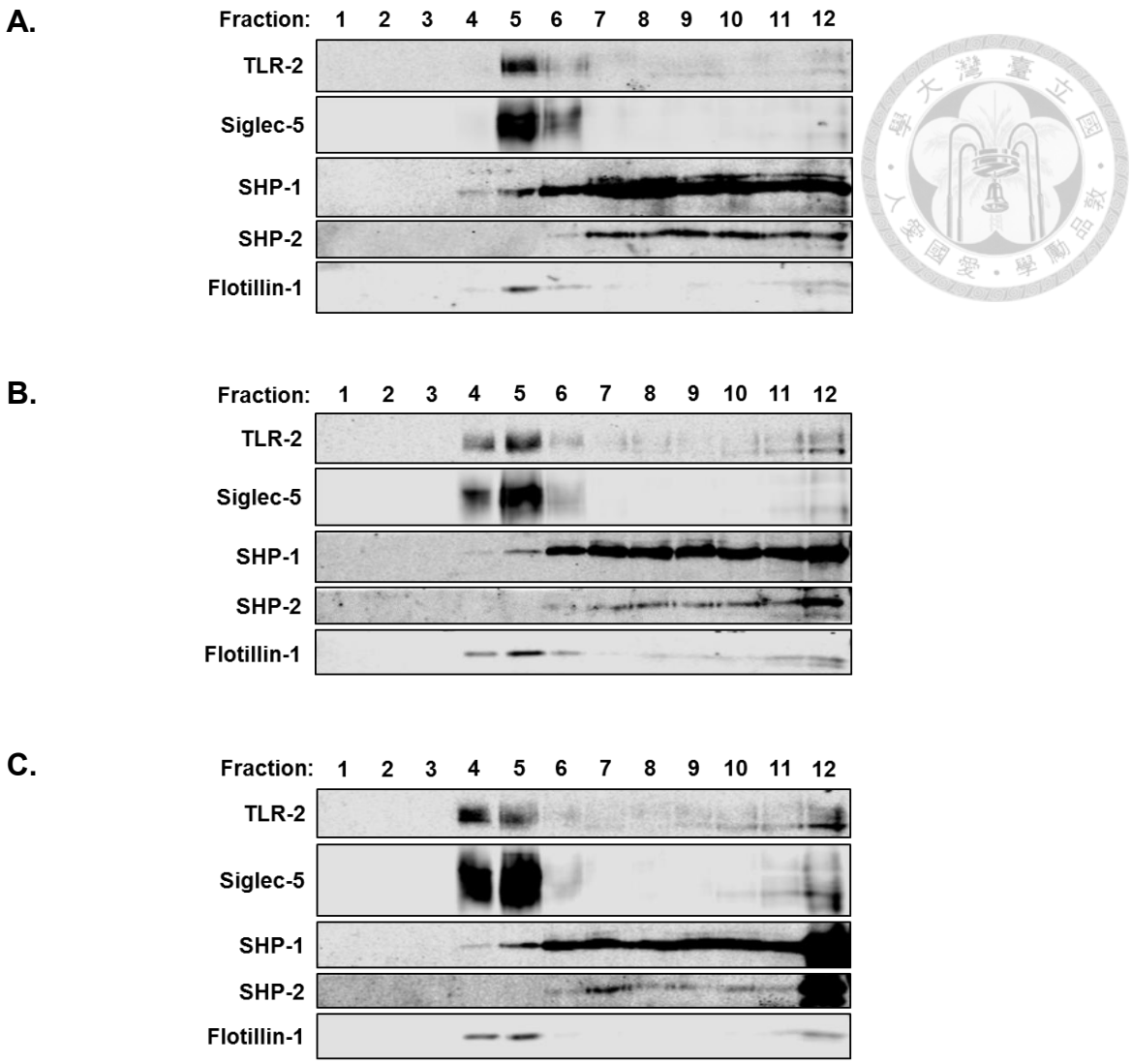

Figure 5. Pneumococcal infection alters the distribution of TLR-2 and Siglec-5 on lipid rafts. Siglec-5 overexpressing THP-1 cells were uninfected (A) or infected with WT (B) or Δ*nanA* (C) SPN at MOI of 10 for 1 hour, followed by sucrose gradient centrifugation to separate raft fractions. Successful raft fractionation was validated by western blot to probe with flotillin-1. The distribution of TLR-2, Siglec-5, SHP-1 and SHP-2 on rafts were then probed with specific antibody recognizing individual target.

doi:10.6342/NTU201701774

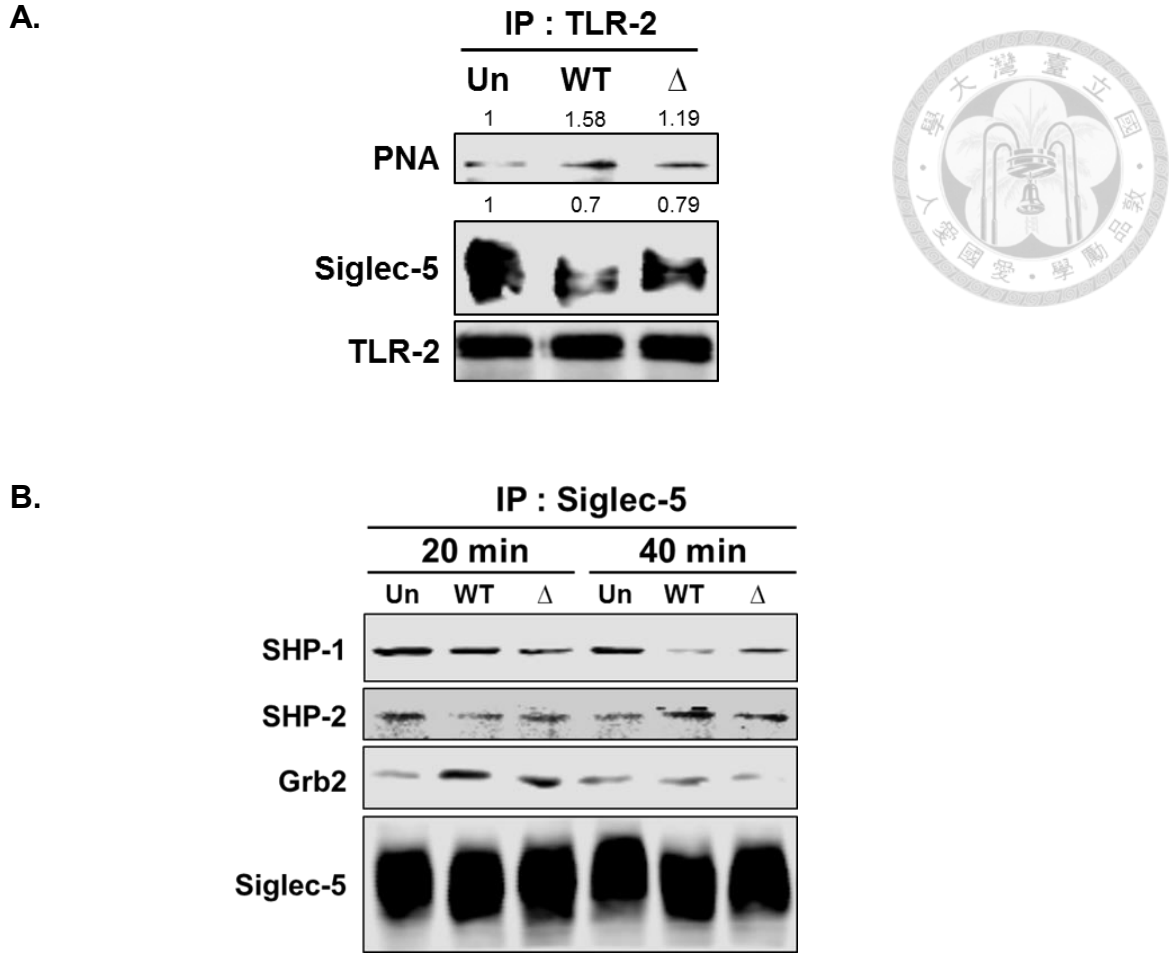

Figure 6. Analysis of the interaction between TLR-2 and Siglec-5 and Siglec-5-associated signaling molecules upon SPN infection. (A) Sig5/THP-1 cells were infected with WT or Δ*nanA* SPN at MOI of 10, and cell lysate was harvested 1 hour after infection and immunoprecipitated with anti-TLR-2 mAb. The precipitates were probed with PNA or antibodies recognizing Siglec-5. (B) To analyze the recruitment of Siglec-5-associated intracellular signaling molecules, Sig5/THP-1 cells were infected with WT or Δ*nanA* SPN at MOI of 10, and cell lysate was harvested 20 min and 40 min after infection and immunoprecipitated with anti-Siglec-5 mAb, followed by probing the precipitates with antibodies recognizing SHP-1, SHP-1 and Grb2.

doi:10.6342/NTU201701774

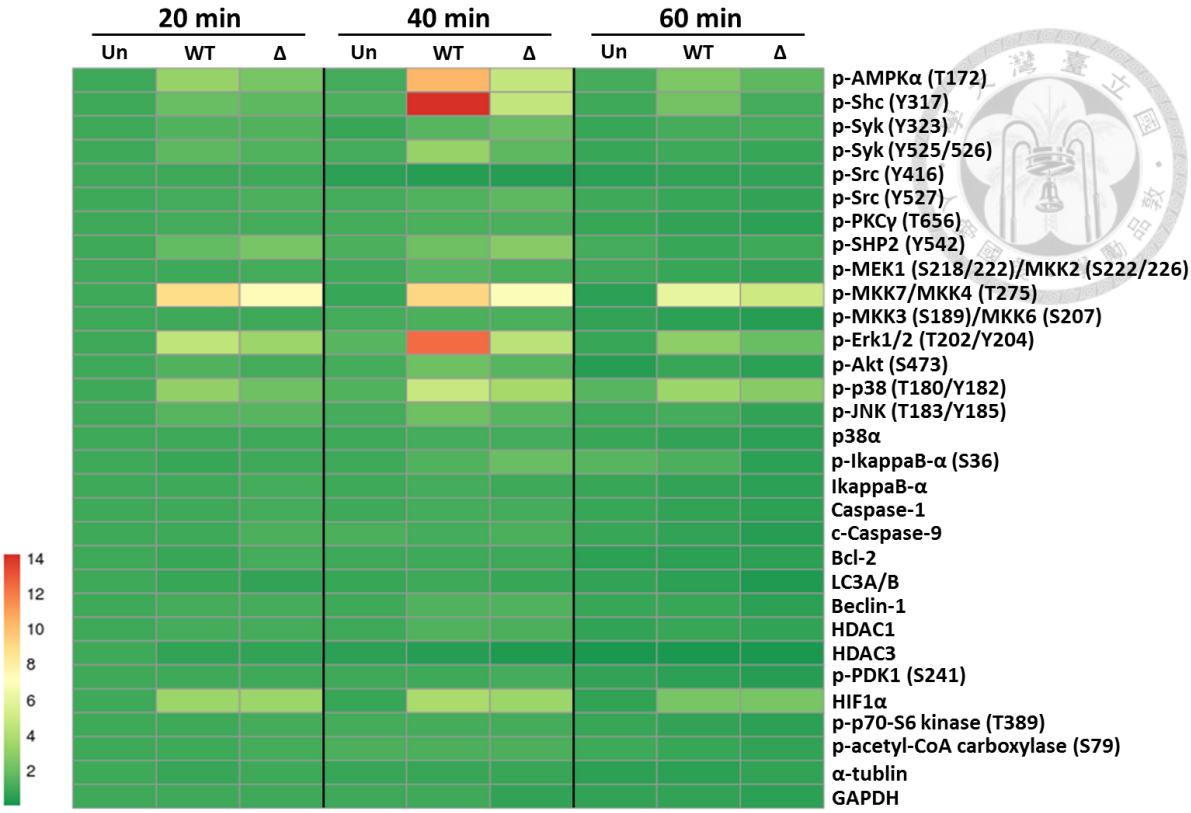

Figure 7. Systematic identification of signaling molecules involved in pneumococcal NanA-provoked cytokine production by Micro-Western Array. THP-1 cells were infected with WT or Δ*nanA* SPN at MOI of 5. Cell lysates were harvested at 20, 40 and 60 min p.i. Image density was quantified by Image Studio Ver 5.2 software and normalized against β-actin. Fold change was calculated as the ratio of each normalized net intensity to the net intensity of uninfected control, followed by log 2 transformation. Heat map was created by R software.

doi:10.6342/NTU201701774

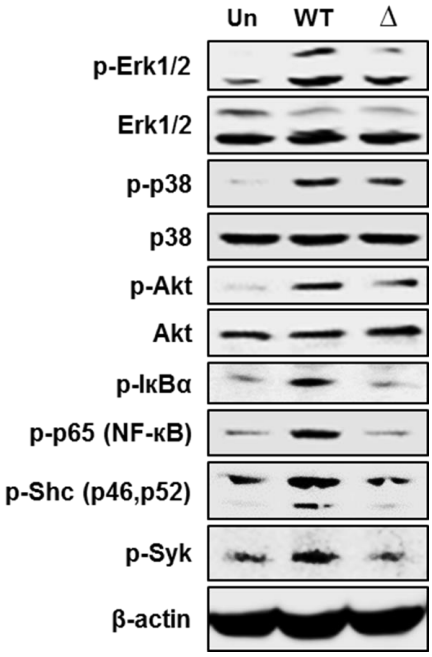

Figure 8. Western blot validation of the selected signaling candidates identified by MWA. THP-1 cells were infected with WT or Δ*nanA* SPN at MOI of 5. Phosphorylation of Shc and Syk was analyzed at 20 min p.i, while phosphorylation of Erk, p38, Akt, IκBα and p65 subunit of NF-κB was analyzed at 60 min p.i. Representative data are shown from two to three independent experiments.

doi:10.6342/NTU201701774

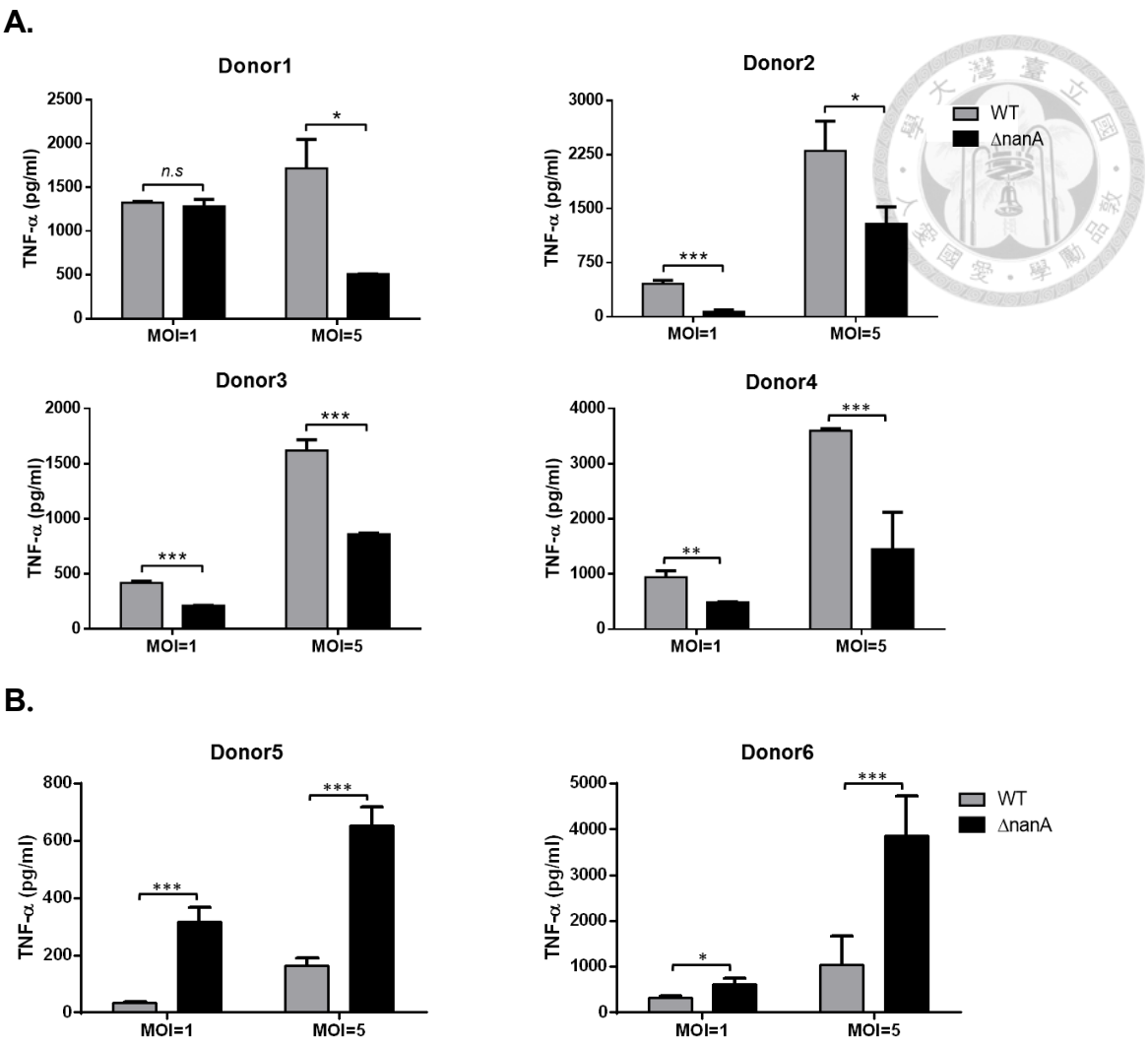

Figure 9. The Siglec-5/-14 genotype influences primary human macrophage responses upon pneumococcal infection. Human $CD14^{+}$ monocyte-derived macrophages from Siglec-$14^{-/-}$ (A) or Siglec-$14^{+/+}$ individuals (B) were infected with WT or Δ*nanA* SPN at MOI of 1 and 5, respectively, for 3 hour. The culture supernatant was collected to perform TNF-α ELISA analysis. Data presented are mean ± SEM and differences between two groups are calculated by 2-tailed *t*-test. * $p<0.05$, ** $p<0.01$, *** $p<0.005$. *n.s*, not significant.

doi:10.6342/NTU201701774

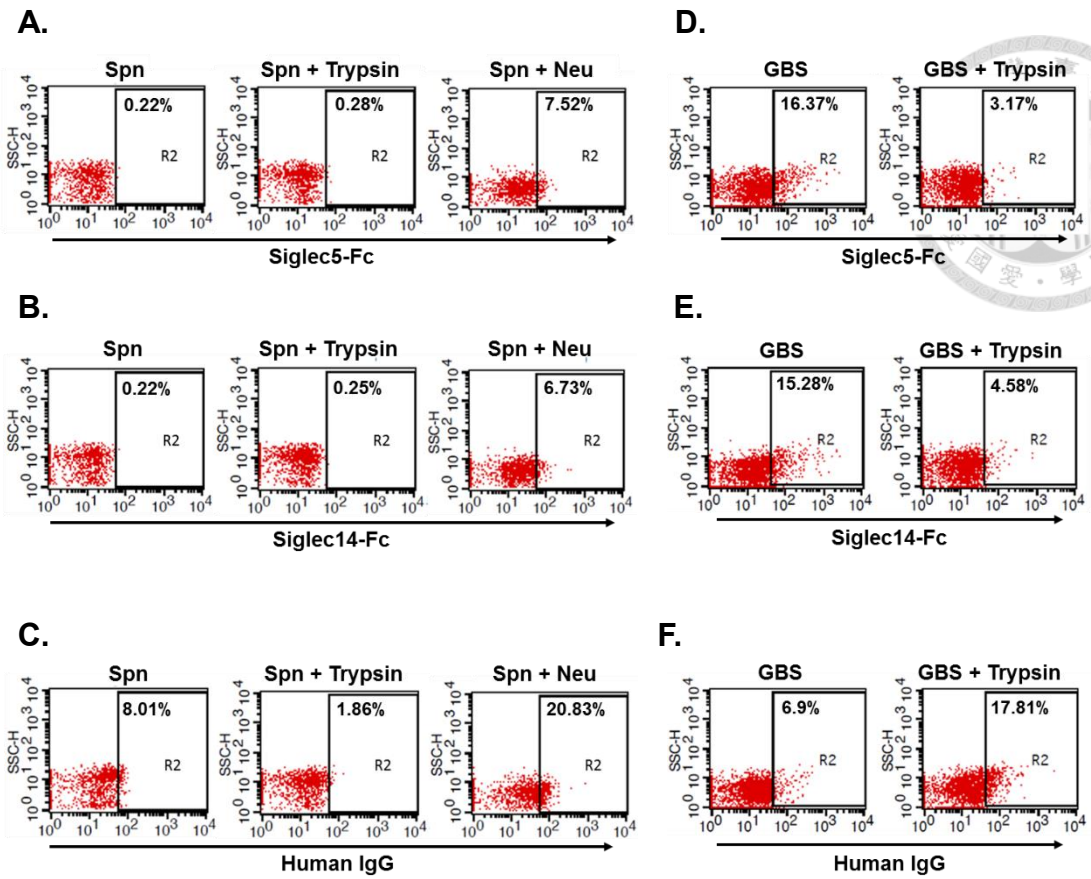

Figure 10. Neither Siglec-5 nor Siglec-14 directly interacts with pneumococcus. Pneumococcus (A, B, C) or group B streptococcus (GBS) A909 strain were pre-treated with 0.25% trypsin or neuraminidase (Neu) and stained with recombinant Siglec5-Fc, Siglec14-Fc or control human IgG, followed by biotinylated goat α-human IgG and APC-conjugated streptavidin. The stained cells were analyzed by flow cytometer.

doi:10.6342/NTU201701774

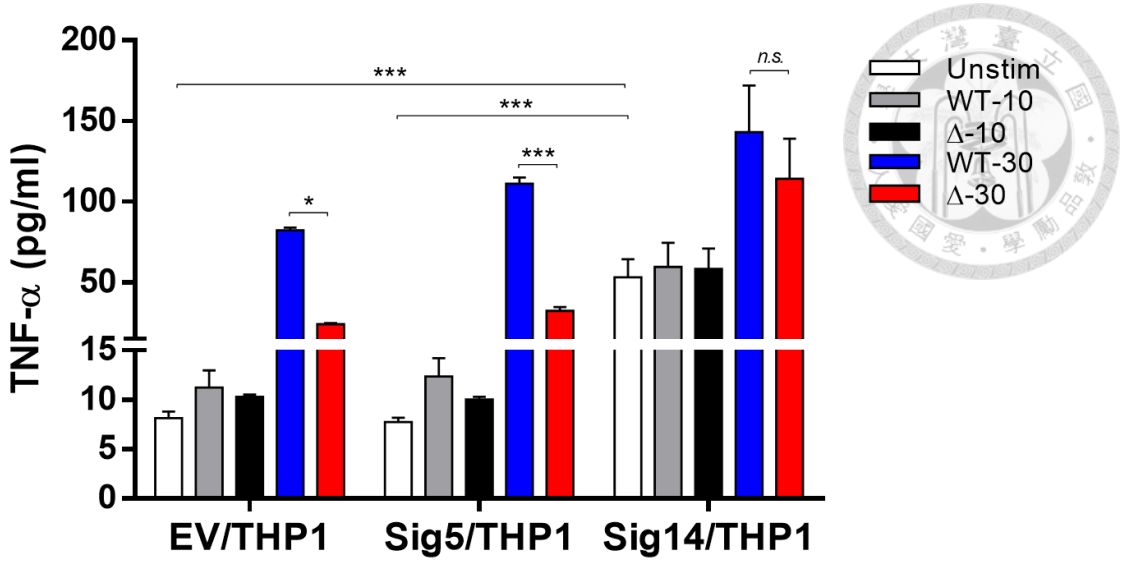

Figure 11. Examination of TNF-α secretion from Siglec-5 and Siglec-14 overexpressing THP-1 upon pneumococcal infection. THP-1 cells stably transfected with empty vector (EV/THP-1), Siglec-5 (Sig5/THP-1) or Siglec-14 (Sig14/THP-1) were infected with WT or Δ*nanA* SPN at MOI of 10 or 30 for 3 hours. The culture supernatant was collected for TNF-α ELISA analysis. Data presented are mean ± SEM. Difference between experimental groups are calculated by one way ANOVA with Turkey's multiple comparisons test. * $p<0.05$, *** $p<0.005$. *n.s*, not significant. Data shown are pooled from two independent experiments.

doi:10.6342/NTU201701774

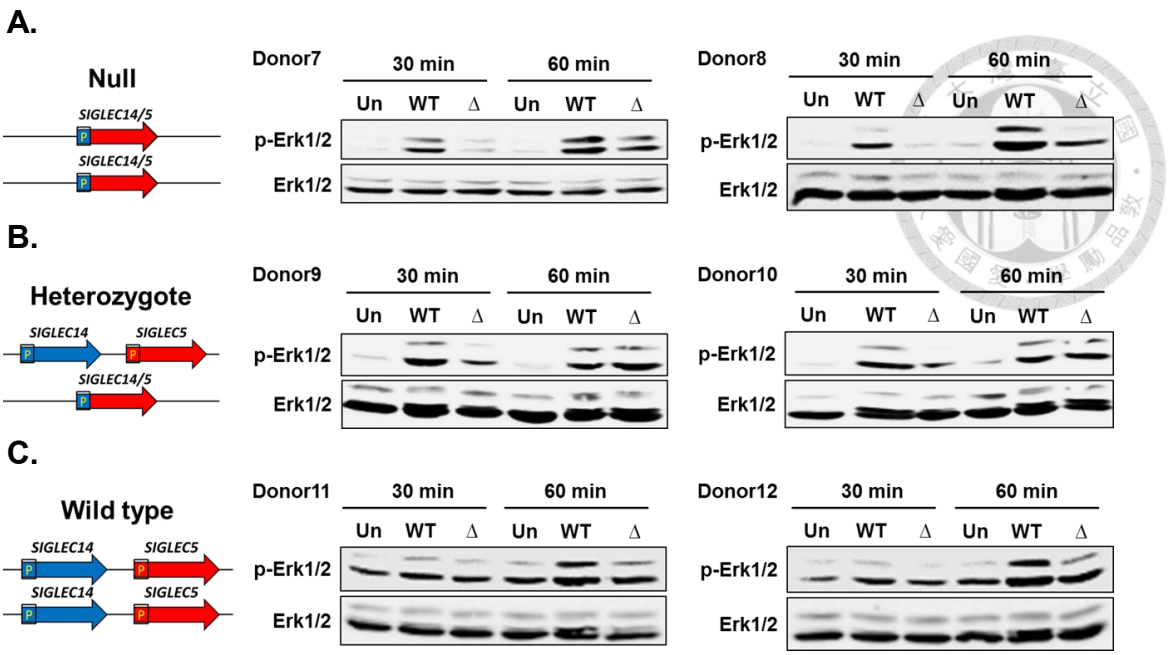

Figure 12. Examination of the phosphorylation of ERK among Siglec-14$^{-/-}$, Siglec-14$^{+/+}$ and Siglec-14$^{+/-}$ individuals upon pneumococcal infection. Human CD14^{+} monocyte-derived macrophages from Siglec-14$^{-/-}$ (A), Siglec-14$^{+/-}$ (B) or Siglec-14$^{+/+}$ (C) individuals were infected with WT or Δ*nanA* SPN at MOI of 5. Phosphorylation of ERK was analyzed at 30 and 60 min p.i. by western blotting.

doi:10.6342/NTU201701774

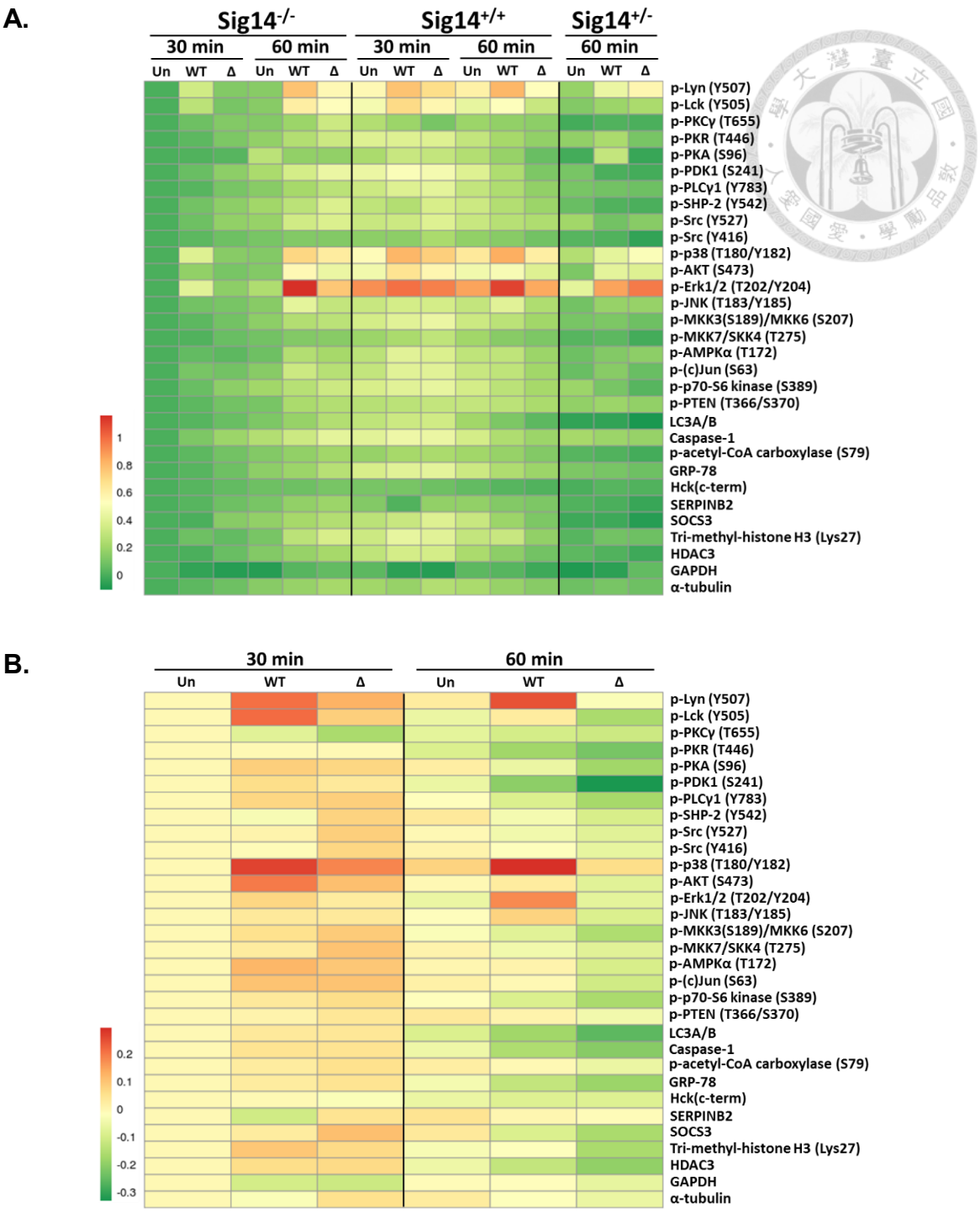

Figure 13. Systematic identification of signaling molecules differed in Siglec-5/-14 genotype upon pneumococcal infection. Human $CD14^{+}$ monocyte-derived macrophages from Siglec-$14^{-/-}$, Siglec-$14^{+/+}$ or Siglec-$14^{+/-}$ individuals were infected with WT or Δ*nanA* SPN at MOI of 5. Cell lysates were harvested at 30 and 60 min p.i, respectively. Image density was quantified by Image Studio Ver 5.2 software and normalized against β-actin. Fold change was calculated as the ratio of each normalized net intensity to the net intensity of uninfected control, followed by log 2 transformation. Heat map was created by R software for all three different Siglec-5/-14 genotype (A) or only for Siglec-$14^{+/+}$ individual (B).

doi:10.6342/NTU201701774

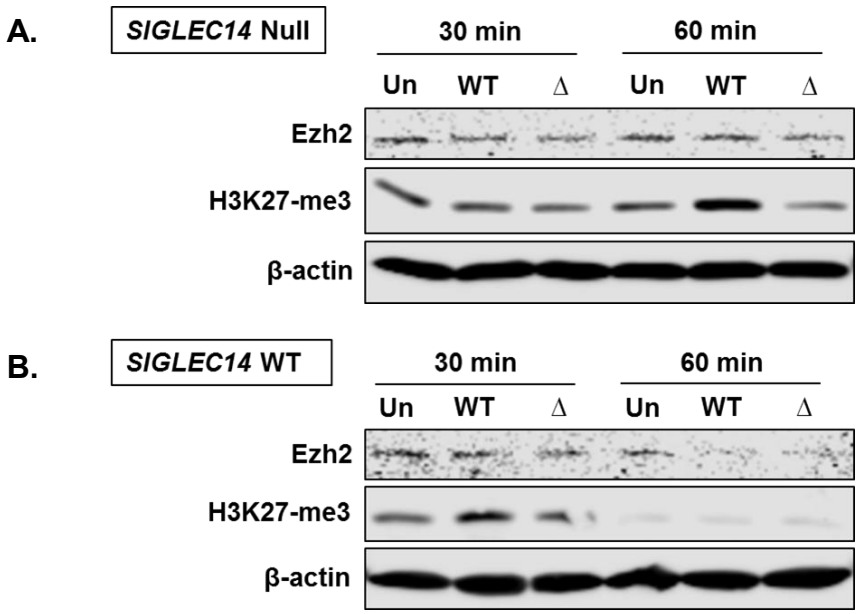

Figure 14. Examination of the expression pattern of Ezh2 and histone 3 Lys27 trimethylation in *SIGLEC14* WT and null individual upon pneumococcal infection. Human $CD14^{+}$ monocyte-derived macrophages from Siglec-$14^{-/-}$ (A) or Siglec-$14^{+/+}$ (B) individuals were infected with WT or Δ*nanA* SPN at MOI of 5. Expression of Ezh2 and H3K27-me3 were analyzed at 30 and 60 min p.i. by western blotting.

doi:10.6342/NTU201701774

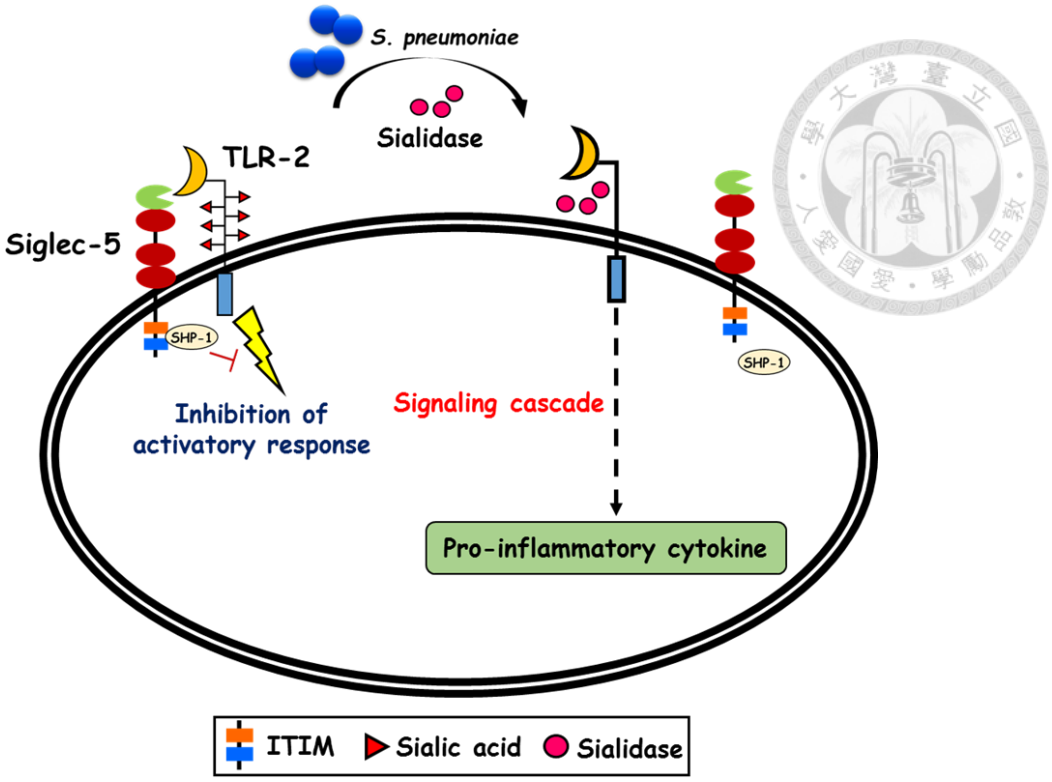

Figure 15. Schematic diagram to demonstrate how NanA-mediated desialylation dysregulates the inflammatory signals and cytokine production upon SPN infection. NanA-mediated desialylation may (1) remove the sialic acids on TLR-2 upon initial contact, (2) disrupt the TLR-2-Siglec interaction, (3) diminish the recruitment of phosphatase to Siglecs, which restrain the downstream signals of TLR-2, and (4) induce exacerbated inflammation.

doi:10.6342/NTU201701774

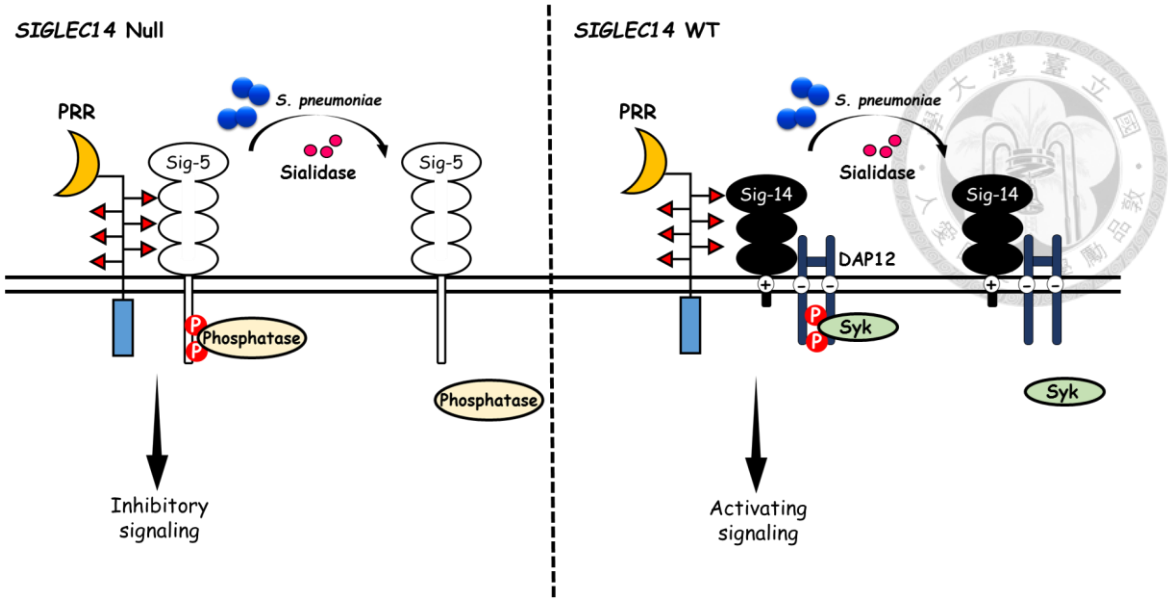

Figure 16. The proposed actions of primary macrophages with different *SIGLEC14* genotypes upon SPN NanA-mediated surface desialylation. Sia *cis*-ligands deliver inhibitory signals through Siglec-5 via the recruited phosphatase activity in Siglec-14 null primary cells. The inhibitory signaling can be interrupted upon SPN-mediated desialylation (left panel). In contrast, Sia *cis*-ligands may deliver tonic activating signals through Siglec-14 via the recruited Syk kinase activity in Siglec-14 WT primary cells. The activating signaling can be interrupted upon SPN-mediated desialylation (right panel).

doi:10.6342/NTU201701774

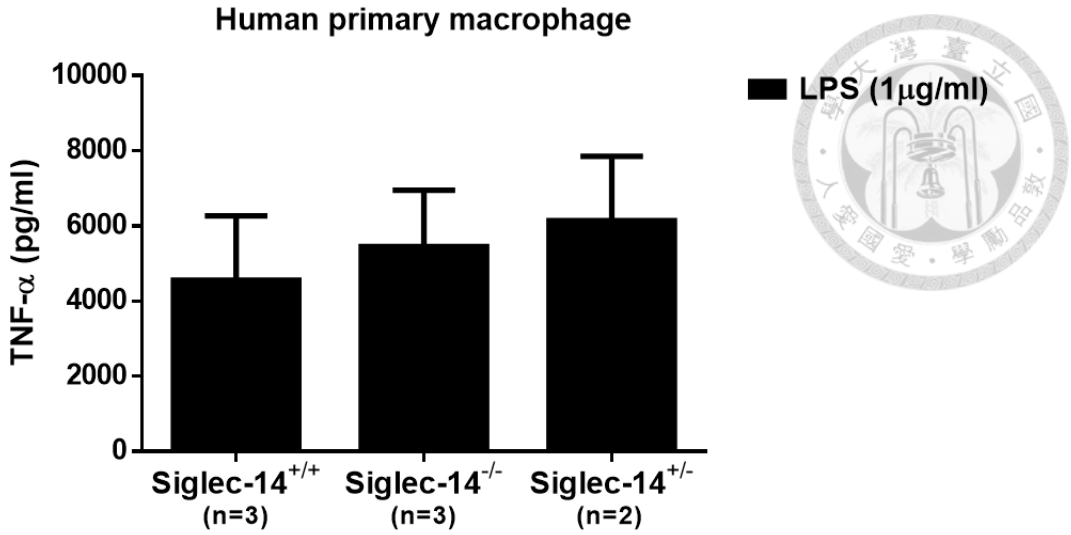

Figure 17. Examination of TNF-α secretion upon LPS stimulation in primary macrophage with different *SIGLEC14* genotypes. Human $CD14^{+}$ monocyte-derived macrophages from Siglec-$14^{+/+}$, Siglec-$14^{-/-}$ or Siglec-$14^{+/-}$ individuals were stimulated with 1μg/ml LPS for 3 hour. The culture supernatant was collected to perform TNF-α ELISA analysis. Data presented are mean ± SEM.

doi:10.6342/NTU201701774

VI. Appendix

Appendix. Table. S1 Summary of structural and functional properties of the Siglec family

Siglec* (other names)	Expression pattern	Structure			Sialoside preference‡	Disease relevance§	Refs
		Number of Ig domains	Tyrosine motifs	DAP12 binding			
Human and mouse sialoadhesin (Siglec-1; CD169)	Macrophages (tissue subsets) and activated monocytes	17	None	No		Autoimmunity and infections including HIV-1, PRRSV, *C. jejuni* and GBS	3,34,35, 44,45, 137,138
Human and mouse CD22 (Siglec-2)	B cells	7	ITIM, ITIM-like and GRB2	No	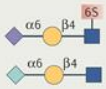	Lymphoma, leukaemia, SLE and rheumatoid arthritis	3,93
Human CD33 (Siglec-3)	Myeloid progenitors, macrophages, monocytes, microglia and granulocytes	2	ITIM and ITIM-like	No		Acute myeloid leukaemia and Alzheimer's disease	3,74–76, 79,80,82, 137,138
Mouse CD33 (Siglec-3)	Macrophages and granulocytes	2	ITIM-like	Unknown	Not determined	Alzheimer's disease	74
Human and mouse MAG (Siglec-4)	Oligodendrocytes and Schwann cells	5	FYN kinase site	No		Neurodegeneration	137,138
Human Siglec-5	Neutrophils, monocytes and B cells	4	ITIM and ITIM-like	No		GBS infection	3,5, 137,139
Human Siglec-6	Trophoblasts and B cells	3	ITIM and ITIM-like	No		Pre-eclampsia	3,138, 140
Human Siglec-7	NK cells, monocytes and mast cells	3	ITIM and ITIM-like	No		Cancer and *C. jejuni* infection	3,42
Human Siglec-8	Eosinophils, mast cells and basophils	3	ITIM and ITIM-like	No		Eosinophilia and asthma	3
Mouse Siglec-F (paralogue of human Siglec-8)	Eosinophils, alveolar macrophages and activated microglia	4	ITIM and ITIM-like	No		Eosinophilia	66,141
Human Siglec-9	Neutrophils, monocytes, DCs and NK cells	3	ITIM and ITIM-like	No		Chronic lung inflammation	3
Mouse Siglec-E (functional orthologue of human Siglec-9)	Neutrophils, monocytes, macrophages and DCs	3	ITIM and ITIM-like	No	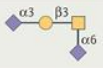	Acute lung injury and neuroinflammation	3,70, 78
Human Siglec-10	B cells, monocytes and eosinophils	5	ITIM, ITIM-like and GRB2	No		Lymphoma, leukaemia, eosinophilia and allergy	3,137, 142
Mouse Siglec-G (orthologue of human Siglec-10)	B cells and myeloid DCs	5	ITIM, ITIM-like and GRB2	No		Tissue damage, sepsis, graft-versus-host disease and autoimmunity	33,40, 41,86, 97,143
Human Siglec-11	Macrophages and microglia	5	ITIM and ITIM-like	No		Neuroinflammation	77,78
Human Siglec-14	Neutrophils and monocytes	3	None	Yes		GBS infection and COPD	5,139
Human and mouse Siglec-15	Osteoclasts, macrophages and DCs	2	None‖	Yes		Osteopetrosis	131
Human Siglec-16	Macrophages and microglia	5	None	Yes		Unknown	8
Mouse Siglec-H	Plasmacytoid DCs and macrophage subsets	2	None	Yes	Not determined	Viral infection and neuroinflammation	3,78, 144–146

C. jejuni, *Campylobacter jejuni*; COPD, chronic obstructive pulmonary disease, DC, dendritic cell; GBS, group B *Streptococcus*; GRB2, growth factor receptor-bound protein 2; Ig, immunoglobulin; ITIM, immunoreceptor tyrosine-based inhibitory motif; MAG, myelin-associated glycoprotein; NK, natural killer; PRRSV, porcine reproductive and respiratory syndrome virus; SLE, systemic lupus erythematosus. *Two additional Siglec genes and proteins are found in chimpanzees that are either only expressed in some humans in a form that does not bind sialic acids (in the case of Siglec-12) or they have been deleted from the human genome (in the case of Siglec-13)[147,148]. ‡Specificities are summarized from the cited references or from glycan array data on the Functional Glycomics Gateway website. Sialoside structures are shown in diagrammatical form showing linkages (indicated by αX and βX, where X is number) between the following residues: *N*-acetylneuraminic acid (purple diamond), *N*-glycolyl-neuraminic acid (light blue diamond), galactose (yellow circle), *N*-acetylgalactosamine (yellow square), *N*-acetylglucosamine (dark blue square), fucose (red triangle). Sulphation is indicated by 'S'. §Disease relevance is based on animal models or expression on cell types that are involved in disease processes. Additional references for disease relevance are cited in the main text. ‖Conserved tyrosine of unknown function.

Nature Reviews Immunology 14, 653–666 (2014)

doi:10.6342/NTU201701774

Appendix. Fig. S1 Siglecs in humans and mice

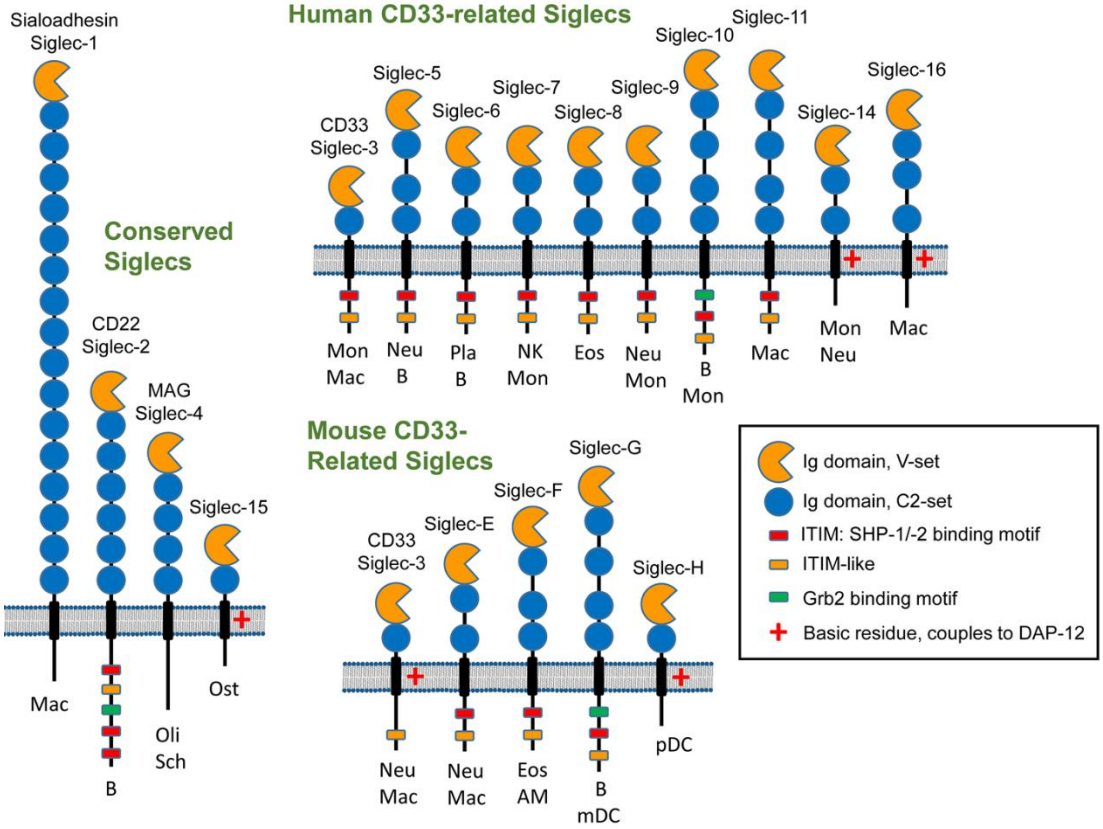

Microbiology Spectrum 4(5), MCHD-0036 (2016)

doi:10.6342/NTU201701774

Appendix. Fig. S2 Signalling mediated by CD22 and the CD33-related Siglecs

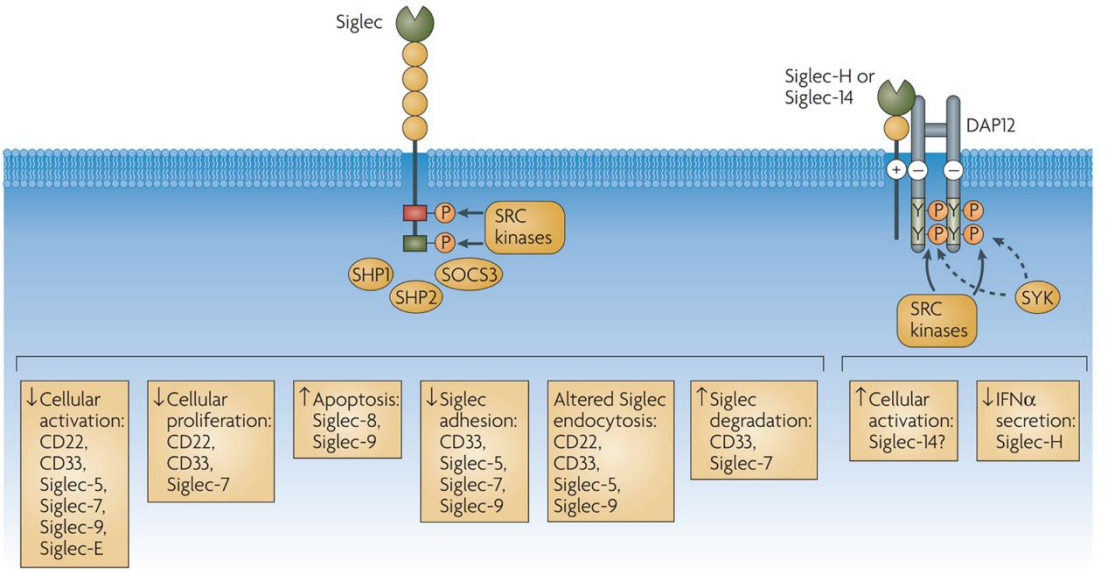

Nature Reviews Immunology 7, 255-266 (2007)

doi:10.6342/NTU201701774

VII. References

1 Adegbola, R. A., Obaro, S. K., Biney, E. & Greenwood, B. M. Evaluation of Binax now *Streptococcus pneumoniae* urinary antigen test in children in a community with a high carriage rate of pneumococcus. *Pediatr Infect Dis J* **20**, 718-719 (2001).

2 Bogaert, D., De Groot, R. & Hermans, P. W. *Streptococcus pneumoniae* colonisation: the key to pneumococcal disease. *The Lancet. Infectious diseases* **4**, 144-154, doi:10.1016/s1473-3099(04)00938-7 (2004).

3 Casey, J. R., Adlowitz, D. G. & Pichichero, M. E. New patterns in the otopathogens causing acute otitis media six to eight years after introduction of pneumococcal conjugate vaccine. *Pediatr Infect Dis J* **29**, 304-309, doi:10.1097/INF.0b013e3181c1bc48 (2010).

4 Kadioglu, A., Weiser, J. N., Paton, J. C. & Andrew, P. W. The role of *Streptococcus pneumoniae* virulence factors in host respiratory colonization and disease. *Nat Rev Microbiol* **6**, 288-301, doi:10.1038/nrmicro1871 (2008).

5 Centers for Disease, C. & Prevention. Direct and indirect effects of routine vaccination of children with 7-valent pneumococcal conjugate vaccine on incidence of invasive pneumococcal disease--United States, 1998-2003. *MMWR Morb Mortal Wkly Rep* **54**, 893-897 (2005).

6 Huang, S. S. *et al.* Post-PCV7 changes in colonizing pneumococcal serotypes in 16 Massachusetts communities, 2001 and 2004. *Pediatrics* **116**, e408-413, doi:10.1542/peds.2004-2338 (2005).

7 Steenhoff, A. P., Shah, S. S., Ratner, A. J., Patil, S. M. & McGowan, K. L. Emergence of vaccine-related pneumococcal serotypes as a cause of bacteremia. *Clin Infect Dis* **42**, 907-914, doi:10.1086/500941 (2006).

8 Pettigrew, M. M., Fennie, K. P., York, M. P., Daniels, J. & Ghaffar, F. Variation in the presence of neuraminidase genes among *Streptococcus pneumoniae* isolates with identical sequence types. *Infect Immun* **74**, 3360-3365, doi:10.1128/IAI.01442-05 (2006).

9 Camara, M., Boulnois, G. J., Andrew, P. W. & Mitchell, T. J. A neuraminidase from *Streptococcus pneumoniae* has the features of a surface protein. *Infection and immunity* **62**, 3688-3695 (1994).

10 King, S. J., Hippe, K. R. & Weiser, J. N. Deglycosylation of human glycoconjugates by the sequential activities of exoglycosidases expressed by *Streptococcus pneumoniae*. *Mol Microbiol* **59**, 961-974, doi:10.1111/j.1365-2958.2005.04984.x (2006).

11 Wren, J. T. *et al.* Pneumococcal Neuraminidase A (NanA) Promotes Biofilm Formation and Synergizes with Influenza A Virus in Nasal Colonization and Middle Ear Infection. *Infect Immun* **85**, doi:10.1128/IAI.01044-16 (2017).

12 Corrales-Medina, V. F. & Musher, D. M. Immunomodulatory agents in the

doi:10.6342/NTU201701774

treatment of community-acquired pneumonia: a systematic review. *J Infect* **63**, 187-199, doi:10.1016/j.jinf.2011.06.009 (2011).

13 Chang, Y. C., Uchiyama, S., Varki, A. & Nizet, V. Leukocyte inflammatory responses provoked by pneumococcal sialidase. *mBio* **3**, doi:10.1128/mBio.00220-11 (2012).

14 Macauley, M. S., Crocker, P. R. & Paulson, J. C. Siglec-mediated regulation of immune cell function in disease. *Nature reviews. Immunology* **14**, 653-666, doi:10.1038/nri3737 (2014).

15 Crocker, P. R., Paulson, J. C. & Varki, A. Siglecs and their roles in the immune system. *Nature reviews. Immunology* **7**, 255-266, doi:10.1038/nri2056 (2007).

16 Ando, M., Tu, W., Nishijima, K. & Iijima, S. Siglec-9 enhances IL-10 production in macrophages via tyrosine-based motifs. *Biochem Biophys Res Commun* **369**, 878-883, doi:10.1016/j.bbrc.2008.02.111 (2008).

17 Ando, M. *et al.* Lectin-dependent localization of cell surface sialic acid-binding lectin Siglec-9. *Cytotechnology* **67**, 601-608, doi:10.1007/s10616-014-9691-6 (2015).

18 Avril, T., Floyd, H., Lopez, F., Vivier, E. & Crocker, P. R. The membrane-proximal immunoreceptor tyrosine-based inhibitory motif is critical for the inhibitory signaling mediated by Siglecs-7 and -9, CD33-related Siglecs expressed on human monocytes and NK cells. *J Immunol* **173**, 6841-6849 (2004).

19 Avril, T., Freeman, S. D., Attrill, H., Clarke, R. G. & Crocker, P. R. Siglec-5 (CD170) can mediate inhibitory signaling in the absence of immunoreceptor tyrosine-based inhibitory motif phosphorylation. *J Biol Chem* **280**, 19843-19851, doi:10.1074/jbc.M502041200 (2005).

20 Sato, S. *et al.* CD22 is both a positive and negative regulator of B lymphocyte antigen receptor signal transduction: altered signaling in CD22-deficient mice. *Immunity* **5**, 551-562 (1996).

21 An, H. *et al.* SHP-2 phosphatase negatively regulates the TRIF adaptor protein-dependent type I interferon and proinflammatory cytokine production. *Immunity* **25**, 919-928, doi:10.1016/j.immuni.2006.10.014 (2006).

22 Hardin, A. O., Meals, E. A., Yi, T., Knapp, K. M. & English, B. K. SHP-1 inhibits LPS-mediated TNF and iNOS production in murine macrophages. *Biochem Biophys Res Commun* **342**, 547-555, doi:10.1016/j.bbrc.2006.02.005 (2006).

23 Kawasaki, N., Rademacher, C. & Paulson, J. C. CD22 regulates adaptive and innate immune responses of B cells. *J Innate Immun* **3**, 411-419, doi:10.1159/000322375 (2011).

24 Ikehara, Y., Ikehara, S. K. & Paulson, J. C. Negative regulation of T cell receptor signaling by Siglec-7 (p70/AIRM) and Siglec-9. *J Biol Chem* **279**, 43117-43125,

doi:10.6342/NTU201701774

doi:10.1074/jbc.M403538200 (2004).

25 Ishida, A. *et al.* Negative regulation of Toll-like receptor-4 signaling through the binding of glycosylphosphatidylinositol-anchored glycoprotein, CD14, with the sialic acid-binding lectin, CD33. *J Biol Chem* **289**, 25341-25350, doi:10.1074/jbc.M113.523480 (2014).

26 Boyd, C. R. *et al.* Siglec-E is up-regulated and phosphorylated following lipopolysaccharide stimulation in order to limit TLR-driven cytokine production. *J Immunol* **183**, 7703-7709, doi:10.4049/jimmunol.0902780 (2009).

27 McMillan, S. J. *et al.* Siglec-E is a negative regulator of acute pulmonary neutrophil inflammation and suppresses CD11b beta2-integrin-dependent signaling. *Blood* **121**, 2084-2094, doi:10.1182/blood-2012-08-449983 (2013).

28 Angata, T., Hayakawa, T., Yamanaka, M., Varki, A. & Nakamura, M. Discovery of Siglec-14, a novel sialic acid receptor undergoing concerted evolution with Siglec-5 in primates. *FASEB journal : official publication of the Federation of American Societies for Experimental Biology* **20**, 1964-1973, doi:10.1096/fj.06-5800com (2006).

29 Angata, T. *et al.* Loss of Siglec-14 reduces the risk of chronic obstructive pulmonary disease exacerbation. *Cellular and molecular life sciences : CMLS* **70**, 3199-3210, doi:10.1007/s00018-013-1311-7 (2013).

30 Ali, S. R. *et al.* Siglec-5 and Siglec-14 are polymorphic paired receptors that modulate neutrophil and amnion signaling responses to group B Streptococcus. *J Exp Med* **211**, 1231-1242, doi:10.1084/jem.20131853 (2014).

31 Fong, J. J. *et al.* Immunomodulatory activity of extracellular Hsp70 mediated via paired receptors Siglec-5 and Siglec-14. *EMBO J* **34**, 2775-2788, doi:10.15252/embj.201591407 (2015).

32 Ono, M., Bolland, S., Tempst, P. & Ravetch, J. V. Role of the inositol phosphatase SHIP in negative regulation of the immune system by the receptor Fc(gamma)RIIB. *Nature* **383**, 263-266, doi:10.1038/383263a0 (1996).

33 Malbec, O. *et al.* Fc epsilon receptor I-associated lyn-dependent phosphorylation of Fc gamma receptor IIB during negative regulation of mast cell activation. *J Immunol* **160**, 1647-1658 (1998).

34 Huang, J. H. *et al.* CR3 and Dectin-1 Collaborate in Macrophage Cytokine Response through Association on Lipid Rafts and Activation of Syk-JNK-AP-1 Pathway. *PLoS Pathog* **11**, e1004985, doi:10.1371/journal.ppat.1004985 (2015).

35 Chen, G. Y., Tang, J., Zheng, P. & Liu, Y. CD24 and Siglec-10 selectively repress tissue damage-induced immune responses. *Science* **323**, 1722-1725, doi:10.1126/science.1168988 (2009).

36 Liu, Y., Chen, G. Y. & Zheng, P. CD24-Siglec G/10 discriminates danger- from pathogen-associated molecular patterns. *Trends Immunol* **30**, 557-561, doi:10.1016/j.it.2009.09.006 (2009).

doi:10.6342/NTU201701774

37 Chen, G. Y. *et al.* Amelioration of sepsis by inhibiting sialidase-mediated disruption of the CD24-SiglecG interaction. *Nat Biotechnol* **29**, 428-435, doi:10.1038/nbt.1846 (2011).

38 Chen, G. Y. *et al.* Broad and direct interaction between TLR and Siglec families of pattern recognition receptors and its regulation by Neu1. *Elife* **3**, e04066, doi:10.7554/eLife.04066 (2014).

39 Yamanaka, M., Kato, Y., Angata, T. & Narimatsu, H. Deletion polymorphism of SIGLEC14 and its functional implications. *Glycobiology* **19**, 841-846, doi:10.1093/glycob/cwp052 (2009).

40 Silva, M. *et al.* Sialic acid removal from dendritic cells improves antigen cross-presentation and boosts anti-tumor immune responses. *Oncotarget* **7**, 41053-41066, doi:10.18632/oncotarget.9419 (2016).

41 Simons, K. & Toomre, D. Lipid rafts and signal transduction. *Nat Rev Mol Cell Biol* **1**, 31-39, doi:10.1038/35036052 (2000).

42 Triantafilou, M., Miyake, K., Golenbock, D. T. & Triantafilou, K. Mediators of innate immune recognition of bacteria concentrate in lipid rafts and facilitate lipopolysaccharide-induced cell activation. *J Cell Sci* **115**, 2603-2611 (2002).

43 Zidovetzki, R. & Levitan, I. Use of cyclodextrins to manipulate plasma membrane cholesterol content: evidence, misconceptions and control strategies. *Biochim Biophys Acta* **1768**, 1311-1324, doi:10.1016/j.bbamem.2007.03.026 (2007).

44 Qu, C. K. The SHP-2 tyrosine phosphatase: signaling mechanisms and biological functions. *Cell Res* **10**, 279-288, doi:10.1038/sj.cr.7290055 (2000).

45 Tamir, I., Dal Porto, J. M. & Cambier, J. C. Cytoplasmic protein tyrosine phosphatases SHP-1 and SHP-2: regulators of B cell signal transduction. *Curr Opin Immunol* **12**, 307-315 (2000).

46 Liu, X. & Qu, C. K. Protein Tyrosine Phosphatase SHP-2 (PTPN11) in Hematopoiesis and Leukemogenesis. *J Signal Transduct* **2011**, 195239, doi:10.1155/2011/195239 (2011).

47 Lowenstein, E. J. *et al.* The SH2 and SH3 domain-containing protein GRB2 links receptor tyrosine kinases to ras signaling. *Cell* **70**, 431-442 (1992).

48 Jellusova, J. & Nitschke, L. Regulation of B cell functions by the sialic acid-binding receptors siglec-G and CD22. *Front Immunol* **2**, 96, doi:10.3389/fimmu.2011.00096 (2011).

49 Jounai, N., Kobiyama, K., Takeshita, F. & Ishii, K. J. Recognition of damage-associated molecular patterns related to nucleic acids during inflammation and vaccination. *Front Cell Infect Microbiol* **2**, 168, doi:10.3389/fcimb.2012.00168 (2012).

50 Tang, D., Kang, R., Coyne, C. B., Zeh, H. J. & Lotze, M. T. PAMPs and DAMPs: signal 0s that spur autophagy and immunity. *Immunol Rev* **249**, 158-175,

doi:10.6342/NTU201701774

doi:10.1111/j.1600-065X.2012.01146.x (2012).

51 Wu, Y., Ren, D. & Chen, G. Y. Siglec-E Negatively Regulates the Activation of TLR4 by Controlling Its Endocytosis. *J Immunol* **197**, 3336-3347, doi:10.4049/jimmunol.1600772 (2016).

52 Le Drean, E. *et al.* Inhibition of antigen-induced T cell response and antibody-induced NK cell cytotoxicity by NKG2A: association of NKG2A with SHP-1 and SHP-2 protein-tyrosine phosphatases. *Eur J Immunol* **28**, 264-276, doi:10.1002/(SICI)1521-4141(199801)28:01<264::AID-IMMU264>3.0.CO;2-O (1998).

53 Kim, E. J., Lee, S. M., Suk, K. & Lee, W. H. CD300a and CD300f differentially regulate the MyD88 and TRIF-mediated TLR signalling pathways through activation of SHP-1 and/or SHP-2 in human monocytic cell lines. *Immunology* **135**, 226-235, doi:10.1111/j.1365-2567.2011.03528.x (2012).

54 Drzeniek, R. Viral and bacterial neuraminidases. *Curr Top Microbiol Immunol* **59**, 35-74 (1972).

55 Jedrzejas, M. J. Pneumococcal virulence factors: structure and function. *Microbiol Mol Biol Rev* **65**, 187-207 ; first page, table of contents, doi:10.1128/MMBR.65.2.187-207.2001 (2001).

56 Air, G. M. & Laver, W. G. The neuraminidase of influenza virus. *Proteins* **6**, 341-356, doi:10.1002/prot.340060402 (1989).

57 Matrosovich, M. N., Matrosovich, T. Y., Gray, T., Roberts, N. A. & Klenk, H. D. Neuraminidase is important for the initiation of influenza virus infection in human airway epithelium. *J Virol* **78**, 12665-12667, doi:10.1128/JVI.78.22.12665-12667.2004 (2004).

58 Cao, H. & Crocker, P. R. Evolution of CD33-related siglecs: regulating host immune functions and escaping pathogen exploitation? *Immunology* **132**, 18-26, doi:10.1111/j.1365-2567.2010.03368.x (2011).

59 Wang, X. *et al.* Evolution of siglec-11 and siglec-16 genes in hominins. *Mol Biol Evol* **29**, 2073-2086, doi:10.1093/molbev/mss077 (2012).

60 Schwarz, F. *et al.* Paired Siglec receptors generate opposite inflammatory responses to a human-specific pathogen. *EMBO J* **36**, 751-760, doi:10.15252/embj.201695581 (2017).

doi:10.6342/NTU201701774